InAs/InP Quantum-Dot Passively Mode-Locked Lasers for 1.55-μm Applications

Ricardo Rosales, Kamel Merghem, Anthony Martinez, A. Akrout, J.-P. Tourrenc, Alain Accard, Francois Lelarge, and Abderrahim Ramdane

(Invited Paper)

***Abstract*—This paper reports on recent results on passively mode-locked InAs/InP quantum-dot-based lasers. These low-dimensional structures have proved very attractive in improving most of the properties of these devices. Subpicosecond pulse generation at repetition rates up to beyond 300 GHz has readily been demonstrated. Ultranarrow RF linewidths reach record values of less than 1 kHz. Controlled optical feedback allows a further reduction of this linewidth yielding extremely low timing jitter. A comparison of single-section and standard two-section lasers is given for the first time. These performances open the way to various applications at 1.55 μm, including very high bit rate all-optical signal processing, frequency comb generation, radio over fiber (RoF), and low-noise all-optical oscillators.**

***Index Terms*—Mode-locked semiconductor lasers, optical pulse generation, quantum dot (QD) lasers.**

I. Introduction

SEMICONDUCTOR monolithic mode-locked lasers (MLL) are very attractive devices for short pulse generation and have found applications in a vast number of fields, including optical telecommunications, microwave photonics, radio over fiber (RoF), optical sampling, biology, and medicine [1], [2]. They have been the subject of numerous investigations since the early demonstration of a semiconductor laser diode, and achieve now unprecedented performance characteristics with pulsewidths in the range of a few hundreds of femtoseconds, repetition rates in excess of 300 GHz at the first harmonic, low timing jitter, and narrow RF linewidths.

Advances in material sciences, in particular, molecular beam epitaxy (MBE) growth, has allowed the achievement of low-dimensional structures including quantum wells (QWs) from which high-performance lasers have been fabricated, particularly contributing to the development of modern optical fiber communication systems. More recently, quantum dot (QD) nanostructures have been grown in which the charge carriers are confined in the three space dimensions. This results in many remarkable properties of directly modulated QD-based lasers and their investigation has witnessed a huge interest in the last decade or so [3].

The first report of a QD-based passive MLL dates back to 2001 [4]. Indeed, some properties of QD lasers are particularly interesting for the mode-locked regime, including low threshold current densities, broad optical gain spectra related to the dot size distribution, potentially low linewidth enhancement factors, ultrafast carrier dynamics, and low optical confinement factors. Most of the achievements have been reported for the InAs/GaAs QD material system that has benefited of much attention. Recent reviews discussing the advantages of using QDs for passively MLLs and related performance are given in [5] and [6] for laser emission at 1.3 μm on GaAs substrates. It is in particular found that the mechanisms for passive mode locking are similar to those of bulk or QW-based standard two-section components consisting of saturable absorber and gain sections [6].

This paper concentrates on passively MLLs intended for the 1.55-μm window, and grown on InP substrates. MBE growth on InP(1 0 0) usually results in the formation of quantum dashes (QDashes) or elongated dots, reported by several groups [7]–[9], while metal–organic vapor phase epitaxy (MOVPE) or chemical beam epitaxy (CBE) growth yields truly 3-D-confined dots [10], [11]. The first reports of QDash-based MLLs emitting at 1.55 μm were for devices consisting of a single-section, so-called "self-pulsating" lasers [12], [13]. QDs obtained by CBE [11] also allow mode locking in single-section devices, while devices based on MOVPE growth present a more conventional behavior in two-section devices where both Q-switching as well as mode locking are reported, depending on operating conditions [10]. The following section describes the growth and type of structures investigated. The results obtained for single-section QDash-based devices will be highlighted in Section III. Subpicosecond pulse generation is hence demonstrated with repetition rates beyond 300 GHz. The mechanism behind pulse generation in these one-section devices will be discussed. Recent study on two-section devices made from an optimized nine-layer QDash design is reported in Section IV. Mode-locking trends in these lasers are compared to those of a reference one-section device made from the same wafer and to the ones reported for InAs/GaAs QD lasers. The use of relatively low confinement

Manuscript received December 1, 2010; revised January 16, 2011; accepted February 7, 2011. This work was supported in part by the French l'Agence Nationale de la Recherche (ANR) through the VERSO "TELDOT" project.

R. Rosales, K. Merghem, A. Martinez, A. Akrout, J. P. Tourrenc, and A. Ramdane are with the Laboratory for Photonics and Nanostructures, 91460 Marcoussis, France (e-mail: ricardo.rosales@lpn.cnrs.fr; Kamel.Merghem@lpn.cnrs.fr; anthony.martinez@lpn.cnrs.fr; akram.akrout@lpn.cnrs.fr; jean.philippe.tourrenc@lpn.cnrs.fr; abderrahim.ramdane@lpn.cnrs.fr).

A. Accard and F. Lelarge are with Alcatel-Thalès III–V Laboratory, 91460 Marcoussis, France (e-mail: alain.accard@3-5lab.fr; francois.lelarge@3-5lab.fr).

Color versions of one or more of the figures in this paper are available online at http://ieeexplore.ieee.org.

Digital Object Identifier 10.1109/JSTQE.2011.2116772

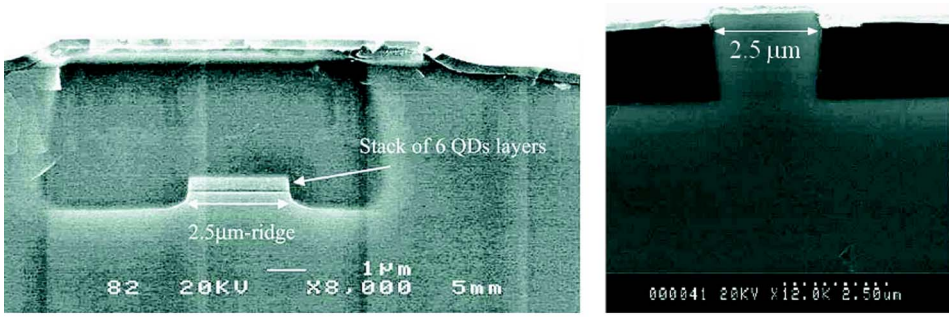

Fig. 1. SEM view of (a) single-mode BRS and (b) shallow-ridge MLL.

factor material systems is advantageous for reducing the phase noise in these devices, owing to the small coupling of the amplified spontaneous emission (ASE) to the propagating mode. This major parameter has been extensively investigated in QDash lasers with a variety of techniques [14], [15] and is discussed in Section V. The effect of controlled feedback to further reduce the phase noise is also reported.

Highlights of a few applications based on these novel devices are presented in Section VI, including all-optical clock recovery at 40 Gb/s [16] and up to 160-Gb/s [17] frequency comb generation for high bit rate wavelength-division multiplexing (WDM) transmission [18] and microwave photonics [19].

II. Growth and Devices

The devices presented in this paper consist of InAs QDash structures grown by gas source MBE (GSMBE) on (1 0 0) InP substrates. The typical dash height and width are ∼2 and ∼20 nm, respectively. Their length ranges from 40 to 300 nm, depending on growth conditions, while their surface density is between 1×10^{10} and 4×10^{10} cm^{-2} [7]. Two types of structures were investigated: dashes in a barrier (DBAR) and dashes in a well (DWELL). The DBAR structure consists of InAs QDashes enclosed within 40-nm-thick barriers and two 80-nm-thick separate confinement heterostructure (SCH) layers. Both the barriers and the SCH are undoped and lattice-matched quaternary $Ga_{0.2}In_{0.8}As_{0.4}P_{0.6}$ layers ($\lambda_g = 1.17$ μm). In the DWELL structure, the QDashes are additionally embedded within 8-nm-thick QWs obtained from a lattice-matched quaternary material emitting at 1.45 μm. The barrier for the QW is again the quaternary $Ga_{0.2}In_{0.8}As_{0.4}P_{0.6}$ material with $\lambda_g = 1.17$ μm. Laser structures have been processed into either ridge waveguide or buried ridge stripe (BRS) lasers (see Fig. 1).

In an earlier study, we have investigated the growth optimization of 6-, 9-, and 12-layer InAs/InP DWELL laser structures [20]. Broad-area laser performance has been investigated as a function of number of layers showing an optimal modal gain for a nine-DWELL layer structure. Fig. 2 shows the threshold current density as a function of reciprocal cavity length for each structure. The Γg_0 modal gain factors are derived from the slope of the curves and amount to 36, 48, and 40 cm^{-1} for 6, 9, and 12 layers, respectively. Moreover, the size distribution of QDashes, illustrated by the room temperature full-width at half-maximum (FWHM), is kept constant from 1 to 12 layers at a value of ∼50 meV.

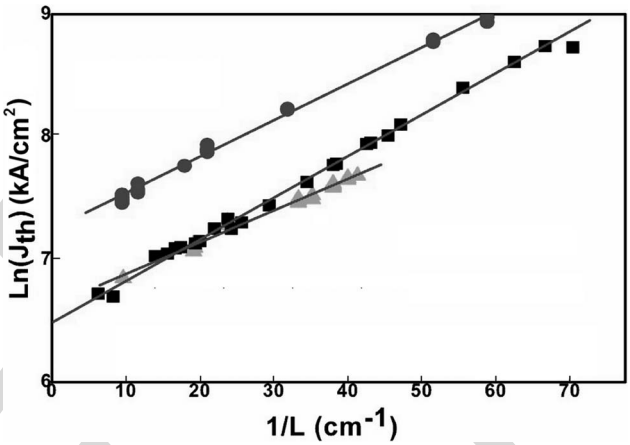

Fig. 2. Threshold current density evolution versus reciprocal cavity length for 6 layers (■), 9 layers (▲), and 12 layers (●) BA lasers. Reprinted with permission from [20].

Exploiting the higher optical confinement factor of multiple layers, which results in a higher modal gain, allowed laser emission for very short cavity lengths. This opens the way to very short pulse generation at extremely high repetition rates in simple one-section device configurations.

III. Short Pulse Generation Using One-Section Fabry–Perot Lasers

In this section, we present mode-locking characteristics of single-section QDash lasers without resorting to an absorber section. The enhanced four-wave mixing (FWM) observed in QDash-based amplifiers [21], [22] appears to be the phenomenon leading to the mode locking in single-section Fabry–Perot (FP) devices. This is attributed to mutual sideband injection due to self-induced carrier density modulation at the longitudinal mode spacing. This process may induce a strong correlation between the phases of longitudinal modes, helping the formation of a pulse train with a repetition rate corresponding to the cavity round-trip time.

Other demonstrations have been reported using one-section FP lasers based on QW [23], [24] and QD active layers [10]. In the latter, Lu *et al.* attribute the passive mode-locking

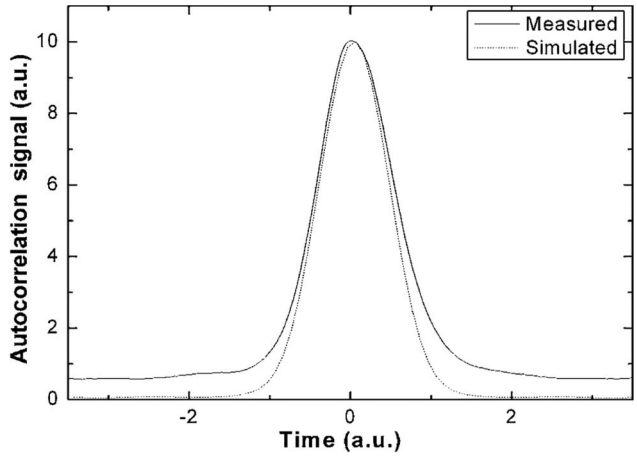

Fig. 3. AC signal of an isolated pulse at 134 GHz for a 340-μm-long QDash FP laser. Reprinted with permission from [13].

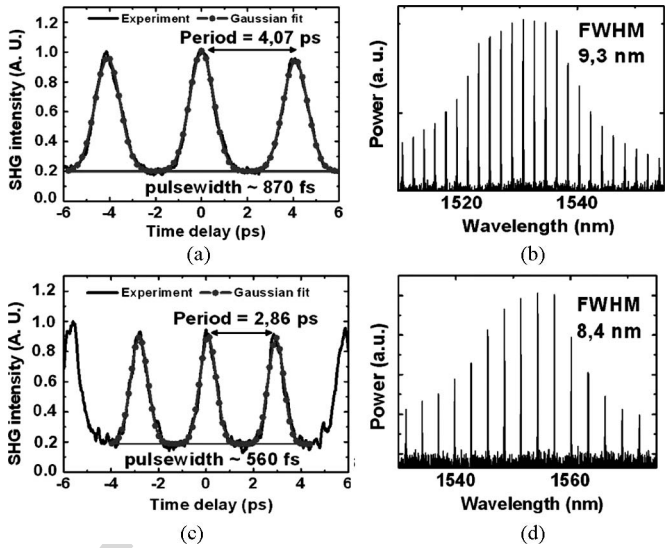

Fig. 4. (a) and (c) AC traces for the 170-μm- and 120-μm-long lasers. (b) and (d) Corresponding optical spectra. Reprinted with permission from [25].

mechanism to large nonlinear optical effects, such as self-phase modulation, cross-phase modulation, and FWM processes within the QD gain cavity.

A semiclassical model for QW self-pulsating FP lasers has been proposed [24] based on a simplified three-mode operation, in which nonlinear dispersion cancel out the mode phase differences induced by the linear dispersion of the gain medium, allowing for ML to establish. A complete model is, however, still needed to account for the many observations reported for both the QW- and QD-based single-section MLLs.

In an earlier study, we have reported transform-limited pulse generation at 134 GHz using a 340-μm-long single-section as-cleaved Fabry-Perot QDash laser diode [13]. Its active core consists of a stack of six InAs QDash layers embedded within InGaAsP QWs (DWELL structure) and separated by InGaAsP barriers. The laser shows a threshold current of 21 mA, with a slope efficiency of 0.12 W/A per facet. A typical autocorrelation (AC) signal of an isolated pulse is shown in Fig. 3. The pulsewidth is measured to be 800 fs after deconvolution assuming a Gaussian profile. Subpicosecond pulses are hence generated without any pulse compression scheme. The time–bandwidth product (TBP) is 0.46, which indicates almost transform-limited pulses.

To achieve even higher repetition rates, optimization of QDash growth has been performed allowing laser emission for cavity lengths down to 120 μm. These optimized structures have been investigated for pulse generation at high repetition rates [25]. In this case, the active region consists of six layers of InAs QDashes enclosed within 40-nm-thick barriers (DBAR) and two 80-nm-thick SCH layers. The laser shows a threshold current of 6 mA, with a slope efficiency of 0.26 W/A per facet. Facets are high reflection coated. Fig. 4 shows a typical AC pulse train for 170-μm- and 120-μm-long lasers corresponding, respectively, to a 245- and 346-GHz repetition rates. After deconvolution of the Gaussian AC profile, we obtained a pulsewidth Δt of 870 fs at 245 GHz [see Fig. 4 (a)]. As the FWHM of the optical spectrum is 9.3 nm for the 170-μm-long laser [see Fig. 4 (b)], the TBP is evaluated to be 1, indicating some residual frequency chirp being present in the pulses. Fig. 4(c) shows the AC signal of the 120-μm-long laser, indicating a repetition period of 2.9 ps (corresponding to 346-GHz repetition rate). The shortest pulsewidth of 560 fs is obtained for a driving current of ~220 mA. Fig. 4(d) shows the corresponding optical spectrum having 8.4 nm width. The TBP was 0.6, close to the Gaussian transform-limited value. Pulses are achieved with peak powers of 100 mW at 245 GHz repetition rate and 20 mW at 346 GHz repetition rate.

One-section lasers show a unique potential, as they allow the achievement of ultrahigh repetition rates without the requirement of a saturable absorber or complex design.

IV. Short Pulse Generation Using Two-Section Devices: A Comparison

Two-section passively MLLs consisting of saturable absorber and gain sections have been extensively investigated in InAs/GaAs QD material systems. These MLLs emitting in the 1.3-μm window have benefited from the broad spectra and ultrafast dynamics in QDs for achieving subpicosecond pulses [5], [6], [26], [27].

While two-section QD-based MLLs results at 1.5 μm are found in the literature [28], [29], their relatively high threshold current densities and waveguide internal losses limit their performance to relatively long pulse durations at low repetition frequencies when compared to their InAs/GaAs counterparts.

In this section, we present for the first time, to our knowledge, high repetition rate two-section passive mode locking at 1.55 μm with comparable performance to that reported for 1.3-μm InAs/GaAs devices. The results are attributed to an optimized structure design that yields broad optical spectra and relatively low threshold currents. The active region consists of nine layers of InAs QDashes separated by InGaAsP barriers. From this dash-in-a-barrier structure, BRS waveguide lasers were processed with a ridge width of 1.5 μm. The as-cleaved one-section

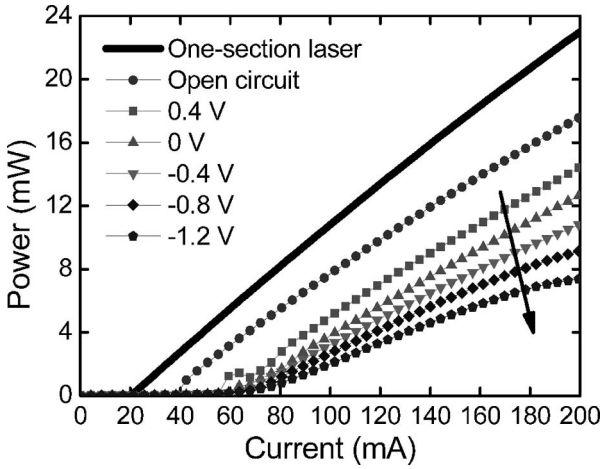

Fig. 5. *L–I* curves for the one-section device and for the two-section device under no bias (open circuit) and applied bias from 0.4 to −1.2 V.

and two-section lasers have a total length of 890 μm, the latter including a 90-μm-long absorber section yielding a repetition rate of 48 GHz in both devices. Threshold currents in the two-section device ranged from 35 mA without biasing the absorber section (open circuit) to 70 mA when a reverse bias of −1.2 V is applied, with corresponding slope efficiencies varying from 0.1 to 0.08 W/A per facet. Corresponding values of 20 and 0.12 W/A are found for the one-section device. Modal gain and internal losses were determined from threshold current versus reciprocal length and slope efficiency versus length curves from broad area (BA) lasers. They have been estimated at 50 and 18 cm^{-1}, respectively. Light–current (*L–I*) characteristics are shown in Fig. 5 for both the one-section and the two-section devices at different absorber bias. Absorption in the smaller section occurs even when forward biased, which explains the lower *L–I* curve at 0.4 V compared to the open-circuit case.

A systematic investigation of ML trends versus operating conditions was carried out. The trends are also compared to those of a single-section laser fabricated from the same wafer and having the same cavity length. The simultaneous effects of gain current and absorber bias on the pulse duration and the FWHM of the optical spectrum are shown in Fig. 6(a) and (b), respectively. Pulse durations were measured by AC through second-harmonic generation with a time resolution of 0.1 ps and assuming secant-hyperbolic pulses. The spectra were measured by an optical spectrum analyzer with a spectral resolution of 0.1 nm. The selected range of driving conditions was found to yield stable mode locking, which smoothly disappears into a continuous wave (CW) or no-lasing regime when driving the laser beyond this region. We notice that mode locking occurs even when forward biasing the absorber section. Fig. 6(a) shows the effects of driving conditions on the pulse duration. Two types of trends are identified when varying the absorber voltage at a fixed drive current. An exponential reduction in pulse duration is observed from the onset of ML at ∼0.4 V down to a value of ∼0 V. Fig. 6(c) shows this trend at 180 mA from 0.3 to −0.1 V where the pulsewidth decreases from 5 to ∼2.5 ps. This is in agreement with experimental and theoretical results for QD

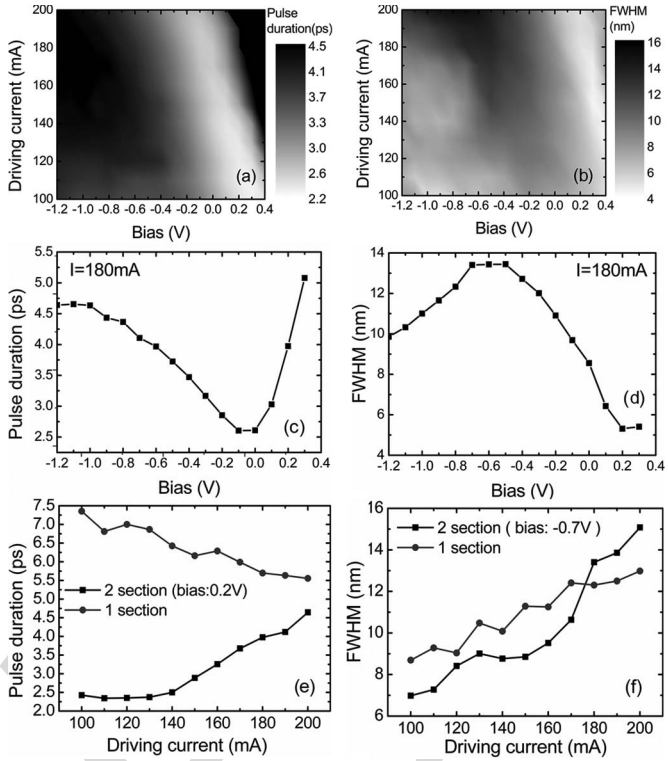

Fig. 6. (a)–(c) Pulse duration and (d)–(f) optical spectrum FWHM as a function of bias and drive current. One-section results are shown in (c) and (f).

MLLs [6], [30]. The opposite trend is observed, if the absorber bias is further decreased to less than ∼0 V. This pulse broadening may be attributed to the quantum-confined stark effect, as described in [31] for QD MLLs, in which a red shift of the absorption spectrum with decreasing bias may result in a reduction of absorption efficiency. As for the case of 1.3-μm QD MLLs, increasing the drive current at a fixed absorber bias has the effect of increasing the pulse duration as seen in Fig. 6(e) at 0.2 V. Interestingly, increasing the driving current in the single-section device results in a reduction of the pulse duration, supporting the assumptions of an ML regime, which relies on intensity-dependent nonlinear interactions. This feature of one-section ML lasers is of great interest since it may allow for the simultaneous achievement of short pulse durations and relatively high average powers. Minimum time–bandwidth products have been evaluated at ∼1.5 and ∼8 for the two-section and single-section lasers, respectively, which indicate chirped pulses. AC traces corresponding to the shortest attainable pulsewidths in both the single- and two-section devices are shown in Fig. 7, obtained for driving currents of 200 mA and 100 mA (at a bias of 0.2 V) yielding ∼5.5 and ∼ 2.5 ps, respectively. For the optical spectrum, the general trend is an increase in the FWHM by decreasing the absorber bias down to an optimum value for a given driving current, as can be seen from Fig. 6(d) at $I =$ 180 mA. The spectral width also increases with drive current, as can be observed in Fig. 6(f) for a fixed absorber bias of −0.7 V. Fig. 6(f) also shows a similar trend for the single-section laser. We attribute this spectral enlargement for both the single- and two-section configurations to band-filling effects due to larger

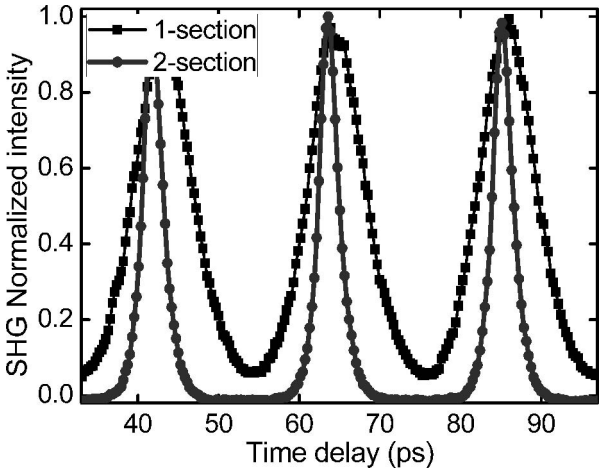

Fig. 7. AC traces for the single- and two-section devices when operating at 200 mA and [100 mA, 0.2 V], respectively.

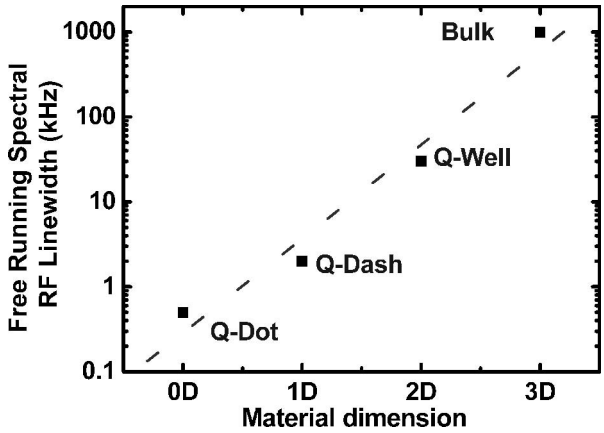

Fig. 8. RF linewidth dependence on material dimensionality. (Adapted from [7].)

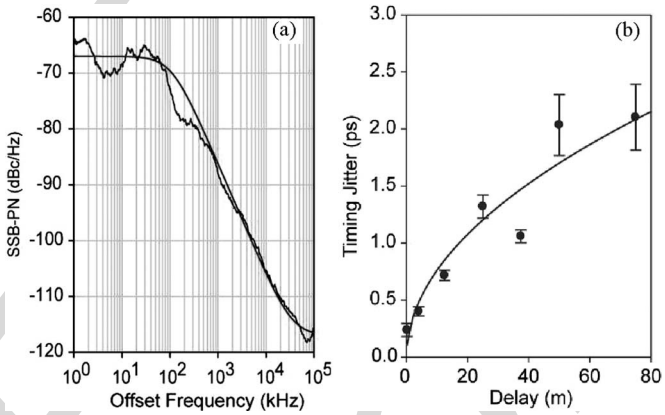

Fig. 9. (a) SSBPN spectral density around the first harmonic of the detected RF signal. (b) Evolution of the timing jitter with increasing delay in the cross-correlation measurement. Solid line: theoretical square-root fit. Reprinted with permission from [14].

carrier densities attainable in this nine-QDash layer active stack. Broad spectral features are desirable for applications such as coherent frequency comb generation for WDM transmission [18]. Both two-section and single-section devices when driven at high injection currents may hence be suitable for this kind of applications. Noise properties were assessed by measuring the RF linewidth of the first harmonic at 48 GHz. Both the single- and the two-section devices exhibited minimum RF linewidths of $\sim$100 kHz.

V. Noise in QDash Passive MLLs

A. Noise in Single-Section QDash Passive MLLs

MLLs are attractive candidates for the generation of stable and periodic pulse trains. They exhibit a potential for applications where small timing jitter is needed. For instance, optical sampling requires a timing jitter of less than 1 ps and even challenging values of 20 fs pulse-to-pulse for an 8-bit 40-Gb/s optical sampler [32]. MLLs characteristics are also potentially valuable in the realization of low-phase-noise oscillators at multigigahertz frequencies for applications in RoF systems [33]. For these purposes, low-dimension QD/Dash-based active materials exhibit unique properties compared to their QW-based counterparts. Indeed, the reduction of the material dimensionality, which implies a lower active volume, results in a lower optical confinement factor [3]; hence, the interaction of the optical guided mode with the ASE is reduced. Moreover, owing to the discrete nature of energy states, the energy diagram of a QD/Dash laser is equivalent to a three-level system [34], where the population inversion factor is close to one. These two properties are responsible for the improved timing jitter performance observed in QD/Dash MLLs. In passively MLLs, the frequency noise of the fundamental harmonic line, measured after photodetection, is mainly induced by spontaneous emission, which represents a source of frequency white noise or equivalently $1/f^2$ phase noise; therefore, the power spectral density of the photocurrent (RF spectrum) is given by a Lorentzian function, whose linewidth is found to be directly linked to the timing jitter [35]. It was shown that the value of the RF linewidth, and therefore, timing jitter, of an MLL is strongly affected by the material system and typically decreases by one order of magnitude when going from bulk to QW and from QW to QD/QDash active regions [7]. Typical values of the RF linewidth lie in the range of a few tens of kilohertz [13] down to a few hundreds of hertz [36], [37] for QD/QDash MLLs compared to several megahertz down to several hundreds of kilohertz for multi-QW MLLs (see Fig. 8), which indicate better timing jitter performance for the QD/Dash-based MLLs.

The timing jitter of passively MLLs is usually evaluated by integrating the single sideband phase noise (SSBPN) spectra in the RF domain. By using this technique, we have measured the timing jitter of single-section QDash MLLs with repetition frequencies of 40 and 10 GHz. The 40-GHz laser is based on a nine-layer InAs/InP DWELL structure. The SSBPN spectrum $L(f)$ measured by an electrical spectrum analyzer and its Lorentzian fit are represented in Fig. 9(a). Integration of the SSBPN was performed between 1 and 20 MHz. Below 1 MHz, the phase noise is affected by low-frequency drifts, and above 20 MHz, by the noise floor level of the ESA as described in [14].

The timing jitter amounts to 0.79 ps, obtained from the measured data, and 0.86 ps using a Lorentzian fit. Its RF linewidth was measured to be 240 kHz.

More recently, optimized active cores with a lower confinement factor have allowed a further reduction in the RF linewidth [37]. These active cores consist of a three-layer stack of InAs QDashes embedded in 40-nm-thick InGaAsP barriers. From this structure, a 10-GHz MLL was processed. A narrow RF linewidth of ∼850 Hz was obtained, leading to a timing jitter of 400 fs in the 150 kHz–50 MHz frequency range. The earlier measurement scheme presents a limitation in determining high-frequency jitter. The limitation arises from the noise floor of the electrical spectrum analyzer, which is reached at some point when increasing the offset frequency. Another limitation comes from the detector and the spectrum analyzer bandwidths, typically around 50 GHz, limiting the repetition frequency range of operation. These limitations are overcome by optical cross-correlation measurements, as described in [38]. This technique has been implemented for measuring the timing jitter in the previously described devices. The experimental setup is presented in [14]. The approach makes use of variable lengths of dispersion-shifted fiber and a controlled fine-delay stage with a 5-fs resolution. Fig. 9(b) shows the evolution of the integrated timing jitter τ_J with increasing delay in the cross-correlation measurement for the 40-GHz MLL. By fitting the data with a square-root function, the timing jitter is found to scale as $\tau_J = 0.201\ L^{1/2}$, with τ_J in units of picoseconds and L in units of meters. The length dependence of τ_J corresponds to the theoretical $1/f^2$ slope of the phase noise in passively MLLs. A timing jitter of 1.08 ps for the frequency interval [1 MHz, 20 MHz] has been evaluated, which is slightly larger than the value of 0.86 ps earlier found by integrating the first harmonic sideband. This technique was also applied to the optimized 10-GHz QDash MLL. A timing jitter of 500 fs in the 150 kHz–50 MHz range has been obtained, which is in good agreement with the value of 400 fs found after SSBPN integration [37].

In this section, we have demonstrated that InAs/InP QDash passive MLLs can exhibit narrow RF linewidths down to less than 1 kHz, implying subpicosend timing jitter values. These remarkable noise performances have been exploited for very high bit rate all-optical signal processing and can be used for low-noise millimeter-wave generation such as in RoF transmission systems (see Section VI).

B. Noise in Two-Section QDash Passive MLLs

First systematic investigations of two-section QDash passive MLLs emitting at 1.5 μm were presented in Section IV for an optimized DBAR structure. Noise trends as a function of driving conditions in these 48-GHz devices were assessed by RF linewidth measurements and compared to those of a one-section device from the same wafer and having same cavity length. Fig. 10(a) shows the dependence of the RF linewidth on the applied bias at currents of 120, 160, and 200 mA. A decrease in the RF linewidth with increasing reverse bias up to an optimum bias point is observed for a given drive current.

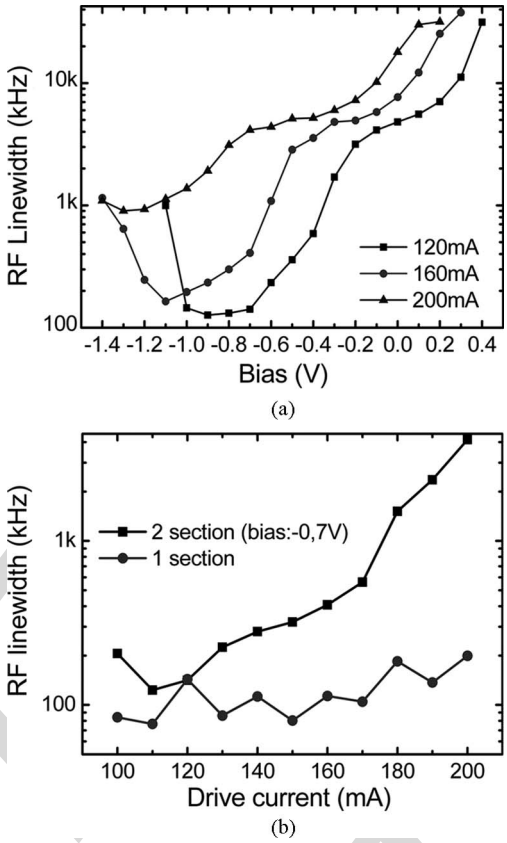

Fig. 10. RF linewidth as a function of (a) absorber bias and (b) driving current.

Fig. 10(b) shows the evolution of the RF linewidth as a function of driving current for both the single- and the two-section devices, the latter when biased at −0.7 V. We note an increase in the RF linewidth with current for the two-section device and a slight change for the one-section laser. These observations may be explained by recognizing that varying the gain section current or the absorber section bias outside their optimal range will alter the balance condition between the effects of gain saturation and saturable absorber that is required for mode locking in two-section devices; hence, a further increase or decrease in bias will result in unstable ML or CW regimes that can be evidenced by an increase in RF linewidth. The RF linewidth increase with current may be attributed to the optical spectrum broadening which results in a scale of ASE spectral bandwidth, and hence, ASE noise, thus increasing the timing phase noise. In general, the one-section device presents a reduced RF linewidth, which may be attributed to lower cavity losses, and hence, reduced phase noise from spontaneous emission. The generally larger RF linewidth observed in two-section devices can, however, be reduced by feedback-stabilization techniques without greatly affecting the pulse durations as described in the following section.

C. Noise Reduction in QDash Passive MLLs

The phase noise of QDash MLLs can be further reduced by means of stabilization techniques based on controlled feedback.

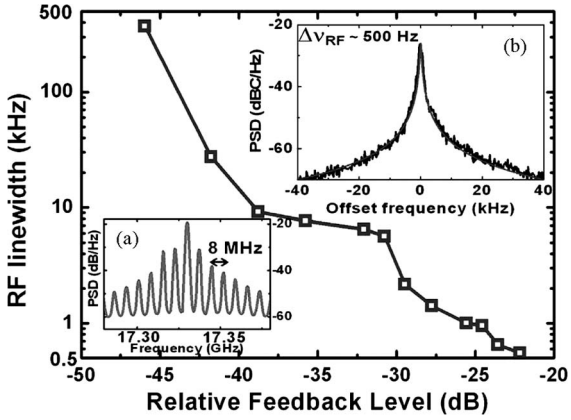

Fig. 11. RF linewidth as a function of the feedback level at a current of 110 mA and a voltage of –1.9 V. Inset (a) RF Spectrum showing harmonic modes separated by 8 MHz. Inset (b) RF spectrum with approximately −22 dB showing an RF linewidth of ∼500 Hz. Reprinted with permission from [40].

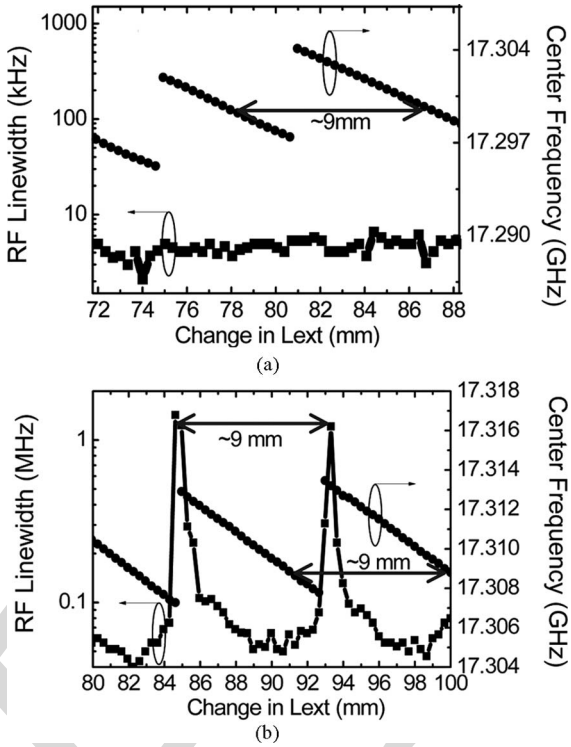

Fig. 12. RF linewidth and center frequency versus external cavity length change for (a) feedback level of approximately −22 dB and (b) feedback level of approximately −40 dB.

This approach has been applied to single-section devices using optoelectronic [19] and optical injection [39] schemes. It has also proven effective in reducing the RF linewidth in conventional two-section QDash MLLs [40] and more recently in InAs/GaAs QD MLLs [41] through optical feedback by using an external optical reflector. In particular, we have investigated the effect of external optical feedback on the pulse duration and RF linewidth of two-section passively MLLs at 17 GHz [40]. In this case, the active region consists of six layers of InAs QDashes. The absorber–gain length ratio of the laser is 4%. We measured the pulse duration and the RF linewidth as a function of gain current and reverse bias with no feedback and under variable feedback levels. Without feedback, pulse duration ranges from 3 to 14 ps, the shortest values being obtained for currents just above threshold. When the laser is subject to a maximum optical feedback of approximately –22 dB, stable mode locking is still observed, even though a reduction of 25% of the mode locking area is evidenced. Without optical feedback, the RF linewidth ranges from 250 kHz to 3.5 MHz. Under the effect of optical feedback, the RF linewidth decreases with feedback level. For instance, for a bias current of 110 mA and a reverse voltage of –1.9 V, the RF linewidth is reduced from 370 kHz (without feedback) down to a record value of 500 Hz with maximum feedback (see Fig. 11), implying a 27-timing jitter reduction [35]. This RF linewidth is comparable to that of high-performance InAs/GaAs QD MLLs [36].

We have also studied the effect of the external cavity length $L_{\rm ext}$ on the RF spectrum by using a delay stage in free space. At strong feedback levels greater than approximately −25 dB, the RF linewidth does not significantly change with $L_{\rm ext}$ [see Fig. 12(a)], whereas at lower feedback ratios [see Fig. 12 (b)], a ∼9-mm periodic dependence is observed. This length introduces a time delay of ∼60 ps in free space, which corresponds to the ML repetition frequency of 17 GHz. This periodicity may suggest an agreement with numerical simulations in [42] where the nonresonant case (i.e., when the ratio between $L_{\rm ext}$ and the laser cavity is irrational) would correspond to the regions of increased RF linewidth in Fig. 12(a). This case may also agree to the unstable dynamics observed by [43] in an InAs/GaAs QD MLL. Fig. 12 also shows the effect on the ML center frequency, showing a periodic dependence also reported in [43].

VI. Highlight of a Few Applications

Owing to their relatively low phase noise characteristics, one-section QDash MLLs have drawn a lot of interest for diverse applications, such as all-optical signal processing and low-noise optoelectronic oscillators (OEOs). Moreover, the wide optical spectrum features combined with the ML performance in these devices represent an advantage in the generation of optical frequency combs. This section reviews published literature related to some of these applications. It is to be noted that these are all single-section MLL-based applications, since high-performance mode locking in two-section devices at 1.5 μm have not been reported up to now.

A. High Bit Rate All-Optical Signal Processing.

All-optical clock recovery at 40 Gb/s has been recently achieved by using a single-section QDash MLL having a repetition frequency of 39.4 GHz [16]. High-frequency jitter suppression of a jittered signal is effectively achieved after injection into the QDash MLL owing to its inherently narrow free-running RF linewidth, which is measured to be 20 kHz when biased at 210 mA. The rms timing jitter of the input signal is reduced from 1.37 to 0.31 ps. The jitter filtering characteristics comply with the ITU-T recommendations. This result paves the way to all-optical clock recovery up to 160 Gb/s.

More recently, all-optical clock recovery performance have been measured at 40, 80, and 160 Gb/s through subharmonic locking mechanism in a 40-GHz one-section QDash FP laser exhibiting a narrow RF linewidth of 10 kHz [17]. Additionally, QDash passively MLLs have been used in wavelength preserving all-optical 3R regenerators at 40 Gb/s [44]. The 3R regenerator includes a single-section QDash MLL laser for low timing jitter clock recovery, which reduces the timing jitter of the input signal from 900 fs to an output timing jitter of less than 550 fs owing to the high-frequency noise-suppression characteristics of the QDash MLL. It is found that the timing jitter of the recovered clock does not change appreciably, as it remains constant at 350 fs for input timing jitters ranging from 400 to 900 fs.

B. Frequency Comb Generation

The inherently wide optical gain spectra related to the inhomogeneous broadening in QDash structures is an asset for frequency comb generation [45]. In addition, the perfect longitudinal mode spacing in QDash MLLs can offer the precise channel separation required in WDM systems, which is otherwise difficult to accomplish. Moreover, due to the ML process, the WDM channels will be coherent, leading to a reduced crosstalk and to an optimal spectral efficiency [46]**.** Error-free transmission of eight separate channels has recently been achieved at 10 Gb/s for a 50-km SMF span, using a 100-GHz QDash-based MLL [18] having a flat optical spectrum of $\sim$10 nm width. The 100-GHz spaced channels are filtered out and launched separately into the fiber. A small measured penalty of $\sim$1.5 dB by using this transmission scheme is shown to arise from the higher relative intensity noise of single longitudinal modes. Bandgap engineering of QDash structures to further widen the optical spectrum remains a key strategy to continue increasing the capacity of WDM systems.

C. Radio Over Fiber

QDash-based MLLs present interesting properties and potential for 60-GHz RoF systems for broadband wireless services. The increase in the demand of bandwidth-hungry multiple services (e.g., multimedia applications such as high-definition TV (HDTV) at bit rates from 1 Gb/s up to 10 Gb/s per user requires the use of transmission techniques of millimeter-wave signals over optical fibers [33], [47].

To ascertain the validity of QDash MLLs for wireless networks, experiments of both frequency up-conversion and distribution, and frequency down-conversion and distribution were carried out over several tens of meters. The radio signal is taken from the IEEE 802 standard [47] with a data rate of 3 Gb/s. The mean error vector magnitude (EVM) was measured to be 10.5% and 15.2% for the up- and down-conversion processes, respectively. The criterion for successful detection being an EVM less than 23%, these experiments validate the ability of the use of single-section QDash lasers for radio-signal transport.

The advantages of 60-GHz QDash MLLs were further assessed in transmission experiments of uncompressed HDTV at a maximum data rate of 3 Gb/s, another major application of broadband RoF technology. It is worth noting that the generation unit consists of a single 60-GHz MLL that can be directly modulated to encode the data onto the signal.

Further improvement of the performances includes the optimization of the direct modulation bandwidth. This implies a simultaneous optimization of the active region for both enhanced mode-locking efficiency and increased direct modulation bandwidth. Such devices are expected to offer a very competitive approach for compact, reduced complexity and cost-effective systems for millimeter-wave generation at the central station for bit rates beyond 10 Gb/s compared to systems using a Mach–Zehnder modulator.

D. Low-Phase-Noise-Coupled Optoelectronic Oscillator

QDash passively MLLs have also been used for the realization of low noise OEOs for millimeter-wave generation [19], [39]. A first demonstration based on a coupled OEO used a 39.9-GHz single-section MLL inserted into two fiber loops. The optical signal is detected by a high-speed photodiode and the resulting electrical signal is fed back into the laser through a bias tee [19]. When the loop is closed, the phase noise is efficiently reduced from –55 dB·c/Hz to –75dB·c/Hz at an offset of 10 kHz and from –75 kHz to –94 dB–c/Hz at an offset of 100 kHz. As the –3-dB modulation bandwidth of the laser was less than 3 GHz, further improvement of the phase noise to comply with system requirements implies reducing the losses of the loops by increasing the modulation efficiency of the QDash laser. As mentioned in part C, practical applications force to perform specific growth optimization both for improved nonlinear effects (i.e., enhanced FWM efficiency) and increased differential gain.

More recently, low phase noise OEO was implemented by means of a 10-GHz QD MLL (RF linewidth $<$ 30 kHz) integrated into a self-injection loop [39]. This makes the whole system simpler and potentially more compact compared to the optoelectronic oscillator that makes use of optoelectronic conversion. When the loop is open, the phase noise exhibits a typical value of –75 dB·c/Hz at an offset of 100 kHz and when the loop is closed its value is reduced to –105 dB·c/Hz, a $\sim$30-dB phase noise reduction. This demonstrates the potential of QDash MLLs inserted into a controlled feedback loop to achieve low-noise oscillators without optoelectronic conversion.

VII. Conclusion

Progress in the growth of self-assembled QDs and QDashes on InP semiconductor substrates has allowed the achievement of high-performance long-wavelength monolithic MLLs. Specific QDash properties, such as inhomogeneous broadening, fast carrier dynamics, and low optical confinement factors have proved valuable assets for ultrashort pulse generation with extremely low noise. Single-section QDash-based FP devices in particular have demonstrated subpicosecond pulsewidths at ultrahigh repetition rates up to 346 GHz. RF linewidths down to a few kilohertz have been reported. Subpicosecond timing jitter in 10- and 40-GHz single-section MLLs was obtained. Controlled optical feedback has allowed to further decrease the RF linewidth to the sub-kHz range in the more standard two-section MLL configuration. There is still room for performance

improvement by fully exploiting the broad optical spectrum. The influence of the type of active region (e.g., DWELL or DBAR) on mode-locking performance will be further investigated. Future developments should also include output power optimization in specific (flared) guided wave configurations.

This should pave the way to a number of applications in the field of not only optical telecommunications but also optical interconnects or microwave photonics. First reported demonstrations based on one-section devices include all-optical clock recovery at up to 160 Gb/s, generation of coherent frequency combs for high bit rate WDM transmission, RoF at 60 GHz for broadband wireless services and extremely low phase noise in all-optical oscillators.

REFERENCES

[1] E. Avrutin, J. Marsh, and E. Portnoi, "Monolithic and multi-GigaHertz mode-locked semiconductor lasers: Constructions, experiments, models and applications," in *Proc. Inst. Elect. Eng., Optoelectron.*, 2000, vol. 147, pp. 251–278.

[2] K. A. Williams, M. G. Thompson, and I. H. White, "Long-wavelength monolithic mode-locked diode lasers," *New J. Phys.*, vol. 6, p. 179, 2004.

[3] D. Bimberg, N. Kirstaedter, N. N. Ledentsov, Z. I. Alferov, P. Kop'ev, and V. M. Ustinov, "InGaAs-GaAs quantum-dot lasers," *IEEE J. Sel. Topics Quantum Electron.*, vol. 3, no. 2, pp. 196–205, Apr. 1997.

[4] X. Huang, A. Stintz, H. Li, L. F. Lester, J. Cheng, and K. J. Malloy, "Passive mode-locking in 1.3 μm two-section InAs quantum dot lasers," *Appl. Phys. Lett.*, vol. 78, pp. 2825–2827, May 2001.

[5] E. U. Rafailov, M. A. Cataluna, and W. Sibbett, "Mode-locked quantum-dot lasers," *Nat. Photon.*, vol. 1, pp. 395–401, Jul. 2007.

[6] M. G. Thompson, A. Rae, X. Mo, R. V. Penty, and I. H. White, "InGaAs quantum-dot mode-locked laser diodes," *IEEE J. Sel. Topics Quantum Electron.*, vol. 15, no. 3, pp. 661–672, Jun. 2009.

[7] F. Lelarge, B. Dagens, J. Renaudier, R. Brenot, A. Accard, F. van Dijk, D. Make, O. Le Gouezigou, J. Provost, F. Poingt, J. Landreau, O. Drisse, E. Derouin, B. Rousseau, F. Pommereau, and G. Duan, "Recent advances on InAs/InP quantum dash based semiconductor lasers and optical amplifiers operating at 1.55 μm," *IEEE J. Sel. Topics Quantum Electron.*, vol. 13, no. 1, pp. 111–124, Jan./Feb. 2007.

[8] R. H. Wang, A. Stintz, P. M. Varangis, T. C. Newell, H. Li, K. J. Malloy, and L. F. Lester, "Room-temperature operation of InAs quantum-dash lasers on InP [001]," *IEEE Photon. Technol. Lett.*, vol. 13, no. 8, pp. 767–769, Aug. 2001.

[9] R. Schwertberger, D. Gold, J. P. Reithmaier, and A. Forchel, "Long-wavelength InP-based quantum-dash lasers," *IEEE Photon. Technol. Lett.*, vol. 14, no. 6, pp. 735–737, Jun. 2002.

[10] Z. G. Lu, J. R. Liu, S. Raymond, P. J. Poole, P. J. Barrios, and D. Poitras, "312-fs pulse generation from a passive C-band InAs/InP quantum dot mode-locked laser," *Opt. Exp.*, vol. 16, pp. 10835–10840, Jul. 2008.

[11] M. J. R. Heck, E. A. J. M. Bente, B. Smalbrugge, Y. Oei, M. K. Smit, S. Anantathanasarn, and R. Notzel, "Observation of Q-switching and mode-locking in two-section InAs/InP (100) quantum dot lasers around 1.55 μm," *Opt. Exp.*, vol. 15, pp. 16292–16301, Dec. 2007.

[12] J. Renaudier, R. Brenot, B. Dagens, F. Lelarge, B. Rousseau, F. Poingt, O. Legouezigou, F. Pommereau, A. Accard, P. Gallion, and G. Duan, "45 GHz self-pulsation with narrow linewidth in quantum dot Fabry-Perot semiconductor lasers at 1.5 μm," *Electron. Lett.*, vol. 41, pp. 1007–1008, 2005.

[13] C. Gosset, K. Merghem, A. Martinez, G. Moreau, G. Patriarche, G. Aubin, A. Ramdane, J. Landreau, and F. Lelarge, "Subpicosecond pulse generation at 134 GHz using a quantum-dash-based Fabry-Perot laser emitting at 1.56 μm," *Appl. Phys. Lett.*, vol. 88, pp. 241105–241113, Jun. 2006.

[14] J. P. Tourrenc, A. Akrout, K. Merghem, A. Martinez, F. Lelarge, A. Shen, G. H. Duan, and A. Ramdane, "Experimental investigation of the timing jitter in self-pulsating quantum-dash lasers operating at 1.55 μm," *Opt. Exp.*, vol. 16, pp. 17706–17713, Oct. 2008.

[15] C. Gosset, K. Merghem, G. Moreau, A. Martinez, G. Aubin, J. Oudar, A. Ramdane, and F. Lelarge, "Phase-amplitude characterization of a high-repetition-rate quantum dash passively mode-locked laser," *Opt. Lett.*, vol. 31, pp. 1848–1850, Jun. 2006.

[16] J. Renaudier, B. Lavigne, F. Lelarge, M. Jourdran, B. Dagens, O. Legouezigou, P. Gallion, and G. Duan, "Standard-compliant jitter transfer function of all-optical clock recovery at 40 GHz based on a quantum-dot self-pulsating semiconductor laser," *IEEE Photon. Technol. Lett.*, vol. 18, no. 11, pp. 1249–1251, Jun. 2006.

[17] V. Roncin, A. O'Hare, S. Lobo, E. Jacquette, L. Bramerie, P. Rochard, Q. Le, M. Gay, J. Simon, A. Shen, J. Renaudier, F. Lelarge, and G. Duan, "Multi-data-rate system performance of a 40-GHz all-optical clock recovery based on a quantum-dot fabry-PÉrot laser," *IEEE Photon. Technol. Lett.*, vol. 19, no. 19, pp. 1409–1411, Oct. 2007.

[18] A. Akrout, A. Shen, R. Brenot, F. Van Dijk, O. Legouezigou, F. Pommereau, F. Lelarge, A. Ramdane, and G. Duan, "Separate error-free transmission of eight channels at 10 Gb/s using comb generation in a quantum-dash-based mode-locked laser," *IEEE Photon. Technol. Lett.*, vol. 21, pp. 1746–1748, 2009.

[19] F. van Dijk, A. Enard, X. Buet, F. Lelarge, and G. Duan, "Phase noise reduction of a quantum dash mode-locked laser in a millimeter-wave coupled opto-electronic oscillator," *J. Lightw. Technol.*, vol. 26, no. 15, pp. 2789–2794, Aug. 2008.

[20] G. Moreau, S. Azouigui, D. Cong, K. Merghem, A. Martinez, G. Patriarche, A. Ramdane, F. Lelarge, B. Rousseau, B. Dagens, F. Poingt, A. Accard, and F. Pommereau, "Effect of layer stacking and p-type doping on the performance of InAs/InP quantum-dash-in-a-well lasers emitting at 1.55 μm," *Appl. Phys. Lett.*, vol. 89, pp. 241123–241125, Dec. 2006.

[21] A. Martinez, G. Aubin, F. Lelarge, R. Brenot, J. Landreau, and A. Ramdane, "Variable optical delays at 1.55 mu m using fast light in an InAs/InP quantum dash based semiconductor optical amplifier," *Appl. Phys. Lett.*, vol. 93, pp. 091116–091118, 2008.

[22] A. Capua, S. O'Duill, V. Mikhelashvili, G. Eisenstein, J. P. Reithmaier, A. Somers, and A. Forchel, "Cross talk free multi channel processing of 10 Gbit/s data via four wave mixing in a 1550 nm InAs/InP quantum dash amplifier," *Opt. Exp.*, vol. 16, pp. 19072–19077, Nov. 2008.

[23] K. Sato, "Optical pulse generation using fabry-Perot lasers under continuous-wave operation," *IEEE J. Sel. Topics Quantum Electron.*, vol. 9, no. 5, pp. 1288–1293, Sep./Oct. 2003.

[24] Y. Nomura, S. Ochi, N. Tomita, K. Akiyama, T. Isu, T. Takiguchi, and H. Higuchi, "Mode locking in Fabry-Perot semiconductor lasers," in *Phys. Rev. A*, Mar. 2002, vol. 65, pp. 043807–043817.

[25] K. Merghem, A. Akrout, A. Martinez, G. Aubin, A. Ramdane, F. Lelarge, and G. Duan, "Pulse generation at 346 GHz using a passively mode locked quantum-dash-based laser at 1.55μm," *Appl. Phys. Lett.*, vol. 94, p. 021107, 2009.

[26] Y. C. Xin, Y. Li, V. Kovanis, A. L. Gray, L. Zhang, and L. F. Lester, "Reconfigurable quantum dot monolithic multisection passive mode-locked lasers," *Opt. Exp.*, vol. 15, pp. 7623–7633, Jun. 2007.

[27] H. Schmeckebier, G. Fiol, C. Meuer, D. Arsenijevi, and D. Bimberg, "Complete pulse characterization of quantum dot mode-locked lasers suitable for optical communication up to 160 Gbit/s," *Opt. Exp.*, vol. 18, pp. 3415–3425, Feb. 2010.

[28] M. J. Heck, E. J. Salumbides, A. Renault, E. A. Bente, Y. Oei, M. K. Smit, R. van Veldhoven, R. Notzel, K. S. Eikema, and W. Ubachs, "Analysis of hybrid mode-locking of two-section quantum dot lasers operating at 1.5 μm," *Opt. Exp.*, vol. 17, pp. 18063–18075, 2009.

[29] C. Lin, Y. Xin, Y. Li, F. L. Chiragh, and L. F. Lester, "Cavity design and characteristics of monolithic long-wavelength InAs/InP quantum dash passively mode-locked lasers," *Opt. Exp.*, vol. 17, pp. 19739–19748, Oct. 2009.

[30] D. B. Malins, A. Gomez-Iglesias, S. J. White, W. Sibbett, A. Miller, and E. U. Rafailov, "Ultrafast electroabsorption dynamics in an InAs quantum dot saturable absorber at 1.3 μm," *Appl. Phys. Lett.*, vol. 89, pp. 171111–171113, 2006.

[31] G. Fiol, C. Meuer, H. Schmeckebier, D. Arsenijevic, S. Liebich, M. Laemmlin, M. Kuntz, and D. Bimberg, "Quantum-Dot semiconductor mode-locked lasers and amplifiers at 40 GHz," *Quantum Electron., IEEE J.*, vol. 45, no. 11, pp. 1429–1435, Nov. 2009.

[32] P. Juodawlkis, J. Twichell, G. Betts, J. Hargreaves, R. Younger, J. Wasserman, F. O'Donnell, K. Ray, and R. Williamson, "Optically sampled analog-to-digital converters," *IEEE Trans. Microw. Theor. Tech.*, vol. 49, no. 10, pp. 1840–1853, Oct. 2001.

[33] A. Vieira, P. Herczfeld, A. Rosen, M. Ermold, E. Funk, W. Jemison, and K. Williams, "A mode-locked microchip laser optical transmitter for fiber radio," *IEEE Trans. Microw. Theor. Tech.*, vol. 49, no. 10, pp. 1882–1887, Oct. 2001.

[34] T. W. Berg and J. Mørk, "Quantum dot amplifiers with high output power and low noise," *Appl. Phys. Lett.*, vol. 82, pp. 3083–3085, 2003.

[35] F. Kefelian, S. O'Donoghue, M. T. Todaro, J. G. McInerney, and G. Huyet, "RF linewidth in monolithic passively mode-locked semiconductor laser," *IEEE Photon. Technol. Lett.*, vol. 20, no. 16, pp. 1405–1407, Aug. 2008.
[36] G. Carpintero, M. G. Thompson, R. V. Penty, and I. H. White, "Low noise performance of passively mode-locked 10-GHz quantum-dot laser diode," *IEEE Photon. Technol. Lett.*, vol. 21, no. 6, pp. 389–391, Mar. 2009.
[37] A. Akrout, K. Merghem, J. P. Tourrenc, A. Martinez, A. Shen, F. Lelarge, G. H. Duan, and A. Ramdane, "Generation of 10 GHz optical pulses with very low timing jitter using one section passively mode locked quantum dash based lasers operating at 1.55 μm," presented at the Opt. Fiber Commun. Conf./Nat. Fiber Opt. Eng. Conf., San Diego, CA, 2009.
[38] L. Jiang, M. Grein, H. Haus, and E. Ippen, "Noise of mode-locked semiconductor lasers," *IEEE J. Sel. Topics Quantum Electron.*, vol. 7, no. 2, pp. 159–167, Apr. 2001.
[39] A. Akrout, A. Shen, A. Enard, G. Duan, F. Lelarge, and A. Ramdane, "Low phase noise all-optical oscillator using quantum dash modelocked laser," *Electron. Lett.*, vol. 46, pp. 73–74, Jan. 2010.
[40] K. Merghem, R. Rosales, S. Azouigui, A. Akrout, A. Martinez, F. Lelarge, G. Duan, G. Aubin, and A. Ramdane, "Low noise performance of passively mode locked quantum-dash-based lasers under external optical feedback," *Appl. Phys. Lett.*, vol. 95, pp. 131111–131113, 2009.
[41] C. Y. Lin, F. Grillot, N. A. Naderi, Y. Li, and L. F. Lester, "Rf linewidth reduction in a quantum dot passively mode-locked laser subject to external optical feedback," *Appl. Phys. Lett.*, vol. 96, pp. 051118–051120, Feb. 2010.
[42] E. A. Avrutin and B. M. Russell, "Dynamics and spectra of monolithic mode-locked laser diodes under external optical feedback," *IEEE J. Quantum Electron.*, vol. 45, no. 11, pp. 1456–1464, Nov. 2009.
[43] F. Grillot, C.-Y. Lin, N. A. Naderi, M. Pochet, and L. F. Lester, "Optical feedback instabilities in a monolithic InAs/GaAs quantum dot passively mode-locked laser," *Appl. Phys. Lett.*, vol. 94, pp. 153503–153505, 2009.
[44] X. Tang, S. H. Chung, J. C. Cartledge, A. Shen, A. Akrout, and G. Duan, "Application of a passively mode-locked quantum-dot Fabry-Perot laser in 40 Gb/s all-optical 3R regeneration," *Opt. Exp.*, vol. 18, pp. 9378–9383, Apr. 2010.
[45] A. Gubenko, I. Krestnikov, D. Livshtis, S. Mikhrin, A. Kovsh, L. West, C. Bornholdt, N. Grote, and A. Zhukov, "Error-free 10 Gbit/s transmission using individual Fabry-Perot modes of low-noise quantum-dot laser," *Electron. Lett.*, vol. 43, pp. 1430–1431, 2007.
[46] T. Healy, F. C. Garcia Gunning, A. D. Ellis, and J. D. Bull, "Multi-wavelength source using low drive-voltage amplitude modulators for optical communications," *Opt. Exp.*, vol. 15, pp. 2981–2986, Mar. 2007.
[47] A. Stöhr, A. Akrout, R. Bub, B. Charbonnier, F. van Dijk, A. Enard, S. Fedderwitz, D. Jäger, M. Huchard, F. Lecoche, J. Marti, R. Sambaraju, A. Steffan, A. Umbach, and M. Weib, "60 GHz radio-over-fiber technologies for broadband wireless services [Invited]," *J. Opt. Netw.*, vol. 8, pp. 471–487, May. 2009.

Ricardo Rosales received the M.Sc. degree in electrical and optical engineering from Telecom SudParis, Evry, France, in 2009. He is currently working toward the Ph.D. degree at the Centre National de la Recherche Scientifique–Laboratory for Photonics and Nanostructures, Marcoussis, France.

His current research interests include semiconductor mode-locked lasers and quantum-dot laser diodes.

Kamel Merghem received the Master's degree in lasers and applications from Université des Sciences et Technologies, Lille, France, in 2000.

He is currently a Research Engineer at the Centre National de la Recherche Scientifique–Laboratory for Photonics and Nanostructures, Marcoussis, France, where he is involved in the research on the fabrication and characterization of semiconductor lasers for telecom applications. His research interests include mode-locked lasers and quantum-dot lasers.

Anthony Martinez was born in 1975. He received the Ph.D. degree in optoelectronics in 2002.

From 2003 to 2005, he was a Postdoctoral Fellow at the Laboratory for Photonics and Nanostructures, where he was the in charge of the design, fabrication and characterizations of high speed lasers based on novel material systems: GaInNAs/GaAs quantum wells and InAs/GaAs quantum dot material for emission at 1.3 μm, and InAs/InP quantum dots/dash operating at 1.55 μm. During 2005, he was a Postdoctoral Fellow at the Center For High Technology Materials (NM), where he was involved in the research on microwave frequency properties of quantum-dot-based lasers. Since 2006, he has been a Permanent Researcher at the Centre National de la Recherche Scientifique–Laboratory for Photonics and Nanostructures, Marcoussis, France. His research interests include photonics components, i.e., semiconductor-based lasers and amplifiers, for telecommunication and defense applications. He has published more than 35 papers in peer-reviewed journals.

A. Akrout, Photograph and biography not available at the time of publication.

J.-P. Tourrenc, Photograph and biography not available at the time of publication.

Alain Accard was born in France, in 1950. He received the M.S. engineer degree in physics from the Institut National des Sciences Appliquees, Lyon, France, in 1975.

He is currently engaged at Alcatel Thales III–V Laboratory, Marcoussis, France. His research interests include Bragg grating design and fabrication of Fabry–Perot and distributed feedback lasers.

Francois Lelarge was born in France, in 1966. He received the Diploma degree in material science and the Ph.D. degree from the University of Pierre et Marie Curie, Paris, France, in 1993 and 1996, respectively.

From 1993 to 1996, he was with the Laboratory of Microstructures and Microelectronic, Centre National de la Recherche Scientifique Bagneux, France. His thesis focused on the fabrication and the optical characterization of GaAs/AlAs lateral supperlattice grown on vicinal surfaces by molecular beam epitaxy. From 1997 to 2000, he was a Postdoctoral Researcher at the Institute of Micro and Optoelectronics, Lausanne, Switzerland, where he was involved in the research on InGaAs/GaAs quantum wires fabrication by metal–organic chemical vapor deposition regrowth on patterned substrates. Currently, he is at Alcatel Thales III–V Laboratory, Marcoussis, France, where he is involved in the research on InGaAsP/InP gas source MBE growth for optoelectronic devices, in particular, on quantum-dots-based lasers and amplifiers.

Abderrahim Ramdane received the Ph.D. degree in semiconductor physics from the University of Nottingham, Nottingham, U.K. in 1981.

He was a Postdoctoral Research Fellow at University of Nottingham for two years, where he was involved in the research on deep levels in III–V compounds. In 1983, he joined the Solar Material Laboratory in Algiers as the Head, where he was involved in the research on single crystal and amorphous silicon solar cells. In 1990, he joined FRANCE TELECOM/Centre National d'Etudes des Télécommunications (CNET Bagneux) as the In Charge of the " Photonic Integrated Circuits on InP" activity. Since 1999, he has been the Director of Research at Centre National de la Recherche Scientifique–Laboratory for Photonics and Nanostructures, Marcoussis, France, where he is engaged in the research on nanostructured optical devices. He has authored or coauthored more than 200 publications in peer reviewed journals and international conferences, and holds five patents in the field of optoelectronic devices.

InAs/InP Quantum-Dot Passively Mode-Locked Lasers for 1.55-μm Applications

Ricardo Rosales, Kamel Merghem, Anthony Martinez, A. Akrout, J.-P. Tourrenc, Alain Accard, Francois Lelarge, and Abderrahim Ramdane

(Invited Paper)

***Abstract*—This paper reports on recent results on passively mode-locked InAs/InP quantum-dot-based lasers. These low-dimensional structures have proved very attractive in improving most of the properties of these devices. Subpicosecond pulse generation at repetition rates up to beyond 300 GHz has readily been demonstrated. Ultranarrow RF linewidths reach record values of less than 1 kHz. Controlled optical feedback allows a further reduction of this linewidth yielding extremely low timing jitter. A comparison of single-section and standard two-section lasers is given for the first time. These performances open the way to various applications at 1.55 μm, including very high bit rate all-optical signal processing, frequency comb generation, radio over fiber (RoF), and low-noise all-optical oscillators.**

***Index Terms*—Mode-locked semiconductor lasers, optical pulse generation, quantum dot (QD) lasers.**

I. Introduction

SEMICONDUCTOR monolithic mode-locked lasers (MLL) are very attractive devices for short pulse generation and have found applications in a vast number of fields, including optical telecommunications, microwave photonics, radio over fiber (RoF), optical sampling, biology, and medicine [1], [2]. They have been the subject of numerous investigations since the early demonstration of a semiconductor laser diode, and achieve now unprecedented performance characteristics with pulsewidths in the range of a few hundreds of femtoseconds, repetition rates in excess of 300 GHz at the first harmonic, low timing jitter, and narrow RF linewidths.

Advances in material sciences, in particular, molecular beam epitaxy (MBE) growth, has allowed the achievement of low-dimensional structures including quantum wells (QWs) from which high-performance lasers have been fabricated, particularly contributing to the development of modern optical fiber communication systems. More recently, quantum dot (QD) nanostructures have been grown in which the charge carriers are confined in the three space dimensions. This results in many remarkable properties of directly modulated QD-based lasers and their investigation has witnessed a huge interest in the last decade or so [3].

The first report of a QD-based passive MLL dates back to 2001 [4]. Indeed, some properties of QD lasers are particularly interesting for the mode-locked regime, including low threshold current densities, broad optical gain spectra related to the dot size distribution, potentially low linewidth enhancement factors, ultrafast carrier dynamics, and low optical confinement factors. Most of the achievements have been reported for the InAs/GaAs QD material system that has benefited of much attention. Recent reviews discussing the advantages of using QDs for passively MLLs and related performance are given in [5] and [6] for laser emission at 1.3 μm on GaAs substrates. It is in particular found that the mechanisms for passive mode locking are similar to those of bulk or QW-based standard two-section components consisting of saturable absorber and gain sections [6].

This paper concentrates on passively MLLs intended for the 1.55-μm window, and grown on InP substrates. MBE growth on InP(1 0 0) usually results in the formation of quantum dashes (QDashes) or elongated dots, reported by several groups [7]–[9], while metal–organic vapor phase epitaxy (MOVPE) or chemical beam epitaxy (CBE) growth yields truly 3-D-confined dots [10], [11]. The first reports of QDash-based MLLs emitting at 1.55 μm were for devices consisting of a single-section, so-called "self-pulsating" lasers [12], [13]. QDs obtained by CBE [11] also allow mode locking in single-section devices, while devices based on MOVPE growth present a more conventional behavior in two-section devices where both Q-switching as well as mode locking are reported, depending on operating conditions [10]. The following section describes the growth and type of structures investigated. The results obtained for single-section QDash-based devices will be highlighted in Section III. Subpicosecond pulse generation is hence demonstrated with repetition rates beyond 300 GHz. The mechanism behind pulse generation in these one-section devices will be discussed. Recent study on two-section devices made from an optimized nine-layer QDash design is reported in Section IV. Mode-locking trends in these lasers are compared to those of a reference one-section device made from the same wafer and to the ones reported for InAs/GaAs QD lasers. The use of relatively low confinement

Manuscript received December 1, 2010; revised January 16, 2011; accepted February 7, 2011. This work was supported in part by the French l'Agence Nationale de la Recherche (ANR) through the VERSO "TELDOT" project.

R. Rosales, K. Merghem, A. Martinez, A. Akrout, J. P. Tourrenc, and A. Ramdane are with the Laboratory for Photonics and Nanostructures, 91460 Marcoussis, France (e-mail: ricardo.rosales@lpn.cnrs.fr; Kamel.Merghem@lpn.cnrs.fr; anthony.martinez@lpn.cnrs.fr; akram.akrout@lpn.cnrs.fr; jean.philippe.tourrenc@lpn.cnrs.fr; abderrahim.ramdane@lpn.cnrs.fr).

A. Accard and F. Lelarge are with Alcatel-Thalès III–V Laboratory, 91460 Marcoussis, France (e-mail: alain.accard@3-5lab.fr; francois.lelarge@3-5lab.fr).

Color versions of one or more of the figures in this paper are available online at http://ieeexplore.ieee.org.

Digital Object Identifier 10.1109/JSTQE.2011.2116772

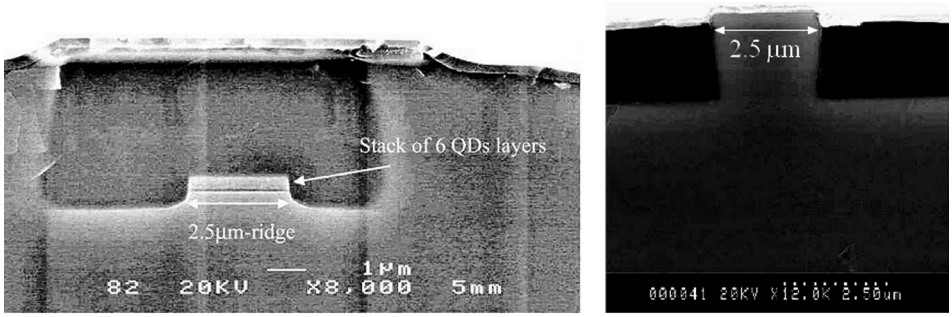

(a) (b)

Fig. 1. SEM view of (a) single-mode BRS and (b) shallow-ridge MLL.

factor material systems is advantageous for reducing the phase noise in these devices, owing to the small coupling of the amplified spontaneous emission (ASE) to the propagating mode. This major parameter has been extensively investigated in QDash lasers with a variety of techniques [14], [15] and is discussed in Section V. The effect of controlled feedback to further reduce the phase noise is also reported.

Highlights of a few applications based on these novel devices are presented in Section VI, including all-optical clock recovery at 40 Gb/s [16] and up to 160-Gb/s [17] frequency comb generation for high bit rate wavelength-division multiplexing (WDM) transmission [18] and microwave photonics [19].

II. Growth and Devices

The devices presented in this paper consist of InAs QDash structures grown by gas source MBE (GSMBE) on (1 0 0) InP substrates. The typical dash height and width are ∼2 and ∼20 nm, respectively. Their length ranges from 40 to 300 nm, depending on growth conditions, while their surface density is between 1×10^{10} and 4×10^{10} cm^{-2} [7]. Two types of structures were investigated: dashes in a barrier (DBAR) and dashes in a well (DWELL). The DBAR structure consists of InAs QDashes enclosed within 40-nm-thick barriers and two 80-nm-thick separate confinement heterostructure (SCH) layers. Both the barriers and the SCH are undoped and lattice-matched quaternary $Ga_{0.2}In_{0.8}As_{0.4}P_{0.6}$ layers ($\lambda_g = 1.17$ μm). In the DWELL structure, the QDashes are additionally embedded within 8-nm-thick QWs obtained from a lattice-matched quaternary material emitting at 1.45 μm. The barrier for the QW is again the quaternary $Ga_{0.2}In_{0.8}As_{0.4}P_{0.6}$ material with $\lambda_g = 1.17$ μm. Laser structures have been processed into either ridge waveguide or buried ridge stripe (BRS) lasers (see Fig. 1).

In an earlier study, we have investigated the growth optimization of 6-, 9-, and 12-layer InAs/InP DWELL laser structures [20]. Broad-area laser performance has been investigated as a function of number of layers showing an optimal modal gain for a nine-DWELL layer structure. Fig. 2 shows the threshold current density as a function of reciprocal cavity length for each structure. The Γg_0 modal gain factors are derived from the slope of the curves and amount to 36, 48, and 40 cm^{-1} for 6, 9, and 12 layers, respectively. Moreover, the size distribution of QDashes, illustrated by the room temperature full-width at half-maximum (FWHM), is kept constant from 1 to 12 layers at a value of ∼50 meV.

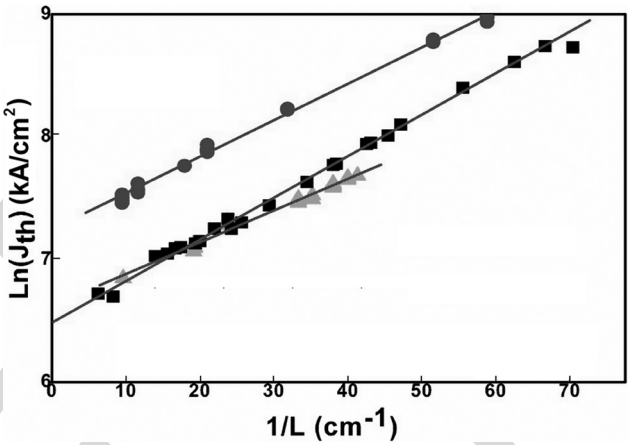

Fig. 2. Threshold current density evolution versus reciprocal cavity length for 6 layers (■), 9 layers (▲), and 12 layers (●) BA lasers. Reprinted with permission from [20].

Exploiting the higher optical confinement factor of multiple layers, which results in a higher modal gain, allowed laser emission for very short cavity lengths. This opens the way to very short pulse generation at extremely high repetition rates in simple one-section device configurations.

III. Short Pulse Generation Using One-Section Fabry–Perot Lasers

In this section, we present mode-locking characteristics of single-section QDash lasers without resorting to an absorber section. The enhanced four-wave mixing (FWM) observed in QDash-based amplifiers [21], [22] appears to be the phenomenon leading to the mode locking in single-section Fabry–Perot (FP) devices. This is attributed to mutual sideband injection due to self-induced carrier density modulation at the longitudinal mode spacing. This process may induce a strong correlation between the phases of longitudinal modes, helping the formation of a pulse train with a repetition rate corresponding to the cavity round-trip time.

Other demonstrations have been reported using one-section FP lasers based on QW [23], [24] and QD active layers [10]. In the latter, Lu *et al.* attribute the passive mode-locking

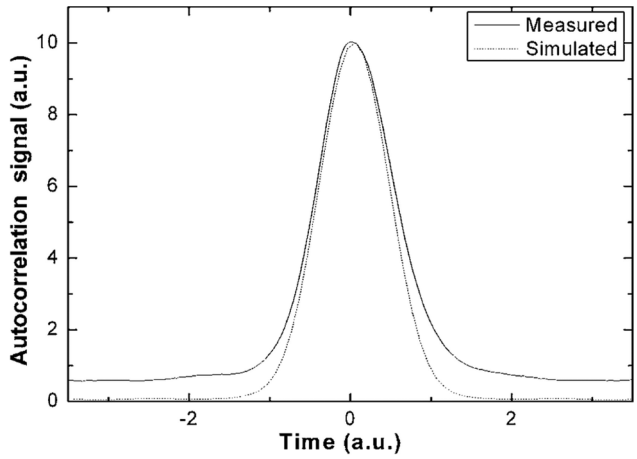

Fig. 3. AC signal of an isolated pulse at 134 GHz for a 340-μm-long QDash FP laser. Reprinted with permission from [13].

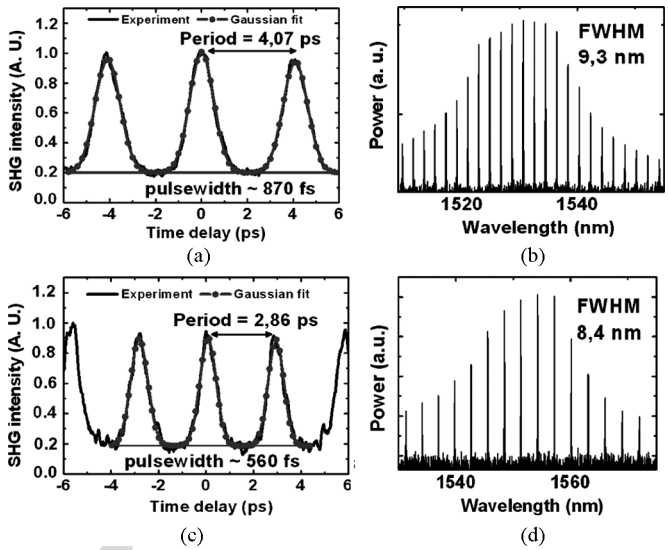

Fig. 4. (a) and (c) AC traces for the 170-μm- and 120-μm-long lasers. (b) and (d) Corresponding optical spectra. Reprinted with permission from [25].

mechanism to large nonlinear optical effects, such as self-phase modulation, cross-phase modulation, and FWM processes within the QD gain cavity.

A semiclassical model for QW self-pulsating FP lasers has been proposed [24] based on a simplified three-mode operation, in which nonlinear dispersion cancel out the mode phase differences induced by the linear dispersion of the gain medium, allowing for ML to establish. A complete model is, however, still needed to account for the many observations reported for both the QW- and QD-based single-section MLLs.

In an earlier study, we have reported transform-limited pulse generation at 134 GHz using a 340-μm-long single-section as-cleaved Fabry-Perot QDash laser diode [13]. Its active core consists of a stack of six InAs QDash layers embedded within InGaAsP QWs (DWELL structure) and separated by InGaAsP barriers. The laser shows a threshold current of 21 mA, with a slope efficiency of 0.12 W/A per facet. A typical autocorrelation (AC) signal of an isolated pulse is shown in Fig. 3. The pulsewidth is measured to be 800 fs after deconvolution assuming a Gaussian profile. Subpicosecond pulses are hence generated without any pulse compression scheme. The time–bandwidth product (TBP) is 0.46, which indicates almost transform-limited pulses.

To achieve even higher repetition rates, optimization of QDash growth has been performed allowing laser emission for cavity lengths down to 120 μm. These optimized structures have been investigated for pulse generation at high repetition rates [25]. In this case, the active region consists of six layers of InAs QDashes enclosed within 40-nm-thick barriers (DBAR) and two 80-nm-thick SCH layers. The laser shows a threshold current of 6 mA, with a slope efficiency of 0.26 W/A per facet. Facets are high reflection coated. Fig. 4 shows a typical AC pulse train for 170-μm- and 120-μm-long lasers corresponding, respectively, to a 245- and 346-GHz repetition rates. After deconvolution of the Gaussian AC profile, we obtained a pulsewidth Δt of 870 fs at 245 GHz [see Fig. 4 (a)]. As the FWHM of the optical spectrum is 9.3 nm for the 170-μm-long laser [see Fig. 4 (b)], the TBP is evaluated to be 1, indicating some residual frequency chirp being present in the pulses. Fig. 4(c) shows the AC signal of the 120-μm-long laser, indicating a repetition period of 2.9 ps (corresponding to 346-GHz repetition rate). The shortest pulsewidth of 560 fs is obtained for a driving current of $\sim$220 mA. Fig. 4(d) shows the corresponding optical spectrum having 8.4 nm width. The TBP was 0.6, close to the Gaussian transform-limited value. Pulses are achieved with peak powers of 100 mW at 245 GHz repetition rate and 20 mW at 346 GHz repetition rate.

One-section lasers show a unique potential, as they allow the achievement of ultrahigh repetition rates without the requirement of a saturable absorber or complex design.

IV. Short Pulse Generation Using Two-Section Devices: A Comparison

Two-section passively MLLs consisting of saturable absorber and gain sections have been extensively investigated in InAs/GaAs QD material systems. These MLLs emitting in the 1.3-μm window have benefited from the broad spectra and ultrafast dynamics in QDs for achieving subpicosecond pulses [5], [6], [26], [27].

While two-section QD-based MLLs results at 1.5 μm are found in the literature [28], [29], their relatively high threshold current densities and waveguide internal losses limit their performance to relatively long pulse durations at low repetition frequencies when compared to their InAs/GaAs counterparts.

In this section, we present for the first time, to our knowledge, high repetition rate two-section passive mode locking at 1.55 μm with comparable performance to that reported for 1.3-μm InAs/GaAs devices. The results are attributed to an optimized structure design that yields broad optical spectra and relatively low threshold currents. The active region consists of nine layers of InAs QDashes separated by InGaAsP barriers. From this dash-in-a-barrier structure, BRS waveguide lasers were processed with a ridge width of 1.5 μm. The as-cleaved one-section

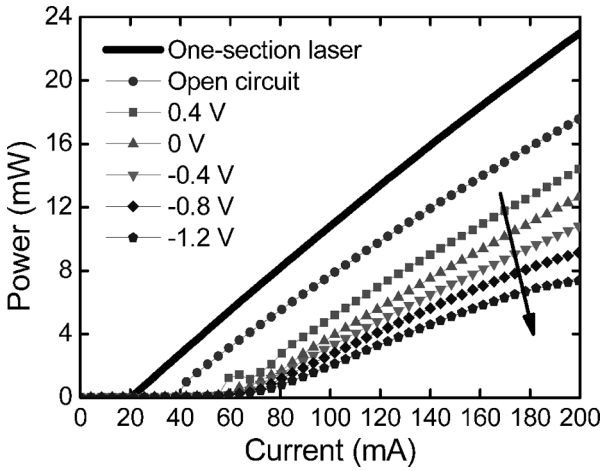

Fig. 5. *L–I* curves for the one-section device and for the two-section device under no bias (open circuit) and applied bias from 0.4 to −1.2 V.

and two-section lasers have a total length of 890 μm, the latter including a 90-μm-long absorber section yielding a repetition rate of 48 GHz in both devices. Threshold currents in the two-section device ranged from 35 mA without biasing the absorber section (open circuit) to 70 mA when a reverse bias of −1.2 V is applied, with corresponding slope efficiencies varying from 0.1 to 0.08 W/A per facet. Corresponding values of 20 and 0.12 W/A are found for the one-section device. Modal gain and internal losses were determined from threshold current versus reciprocal length and slope efficiency versus length curves from broad area (BA) lasers. They have been estimated at 50 and 18 cm^{-1}, respectively. Light–current (*L–I*) characteristics are shown in Fig. 5 for both the one-section and the two-section devices at different absorber bias. Absorption in the smaller section occurs even when forward biased, which explains the lower *L–I* curve at 0.4 V compared to the open-circuit case.

A systematic investigation of ML trends versus operating conditions was carried out. The trends are also compared to those of a single-section laser fabricated from the same wafer and having the same cavity length. The simultaneous effects of gain current and absorber bias on the pulse duration and the FWHM of the optical spectrum are shown in Fig. 6(a) and (b), respectively. Pulse durations were measured by AC through second-harmonic generation with a time resolution of 0.1 ps and assuming secant-hyperbolic pulses. The spectra were measured by an optical spectrum analyzer with a spectral resolution of 0.1 nm. The selected range of driving conditions was found to yield stable mode locking, which smoothly disappears into a continuous wave (CW) or no-lasing regime when driving the laser beyond this region. We notice that mode locking occurs even when forward biasing the absorber section. Fig. 6(a) shows the effects of driving conditions on the pulse duration. Two types of trends are identified when varying the absorber voltage at a fixed drive current. An exponential reduction in pulse duration is observed from the onset of ML at ∼0.4 V down to a value of ∼0 V. Fig. 6(c) shows this trend at 180 mA from 0.3 to −0.1 V where the pulsewidth decreases from 5 to ∼2.5 ps. This is in agreement with experimental and theoretical results for QD

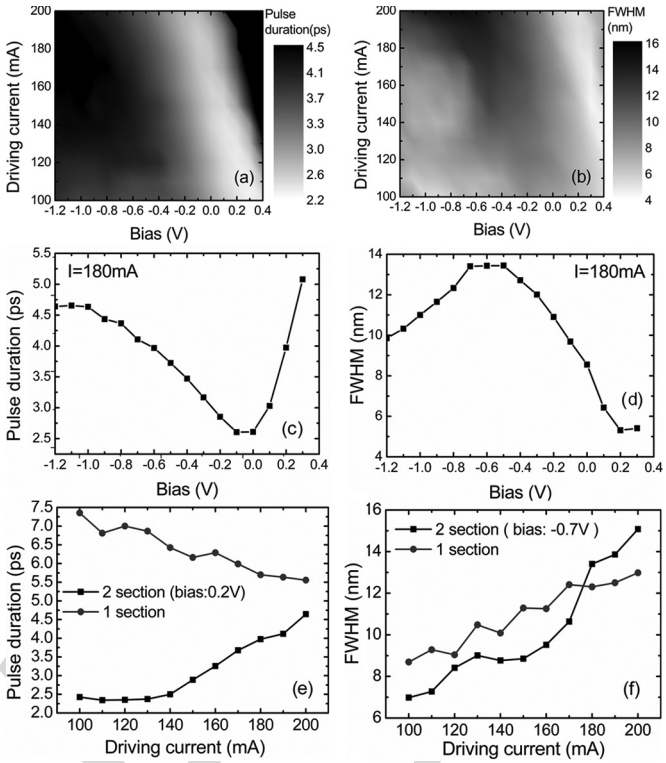

Fig. 6. (a)–(c) Pulse duration and (d)–(f) optical spectrum FWHM as a function of bias and drive current. One-section results are shown in (c) and (f).

MLLs [6], [30]. The opposite trend is observed, if the absorber bias is further decreased to less than ∼0 V. This pulse broadening may be attributed to the quantum-confined stark effect, as described in [31] for QD MLLs, in which a red shift of the absorption spectrum with decreasing bias may result in a reduction of absorption efficiency. As for the case of 1.3-μm QD MLLs, increasing the drive current at a fixed absorber bias has the effect of increasing the pulse duration as seen in Fig. 6(e) at 0.2 V. Interestingly, increasing the driving current in the single-section device results in a reduction of the pulse duration, supporting the assumptions of an ML regime, which relies on intensity-dependent nonlinear interactions. This feature of one-section ML lasers is of great interest since it may allow for the simultaneous achievement of short pulse durations and relatively high average powers. Minimum time–bandwidth products have been evaluated at ∼1.5 and ∼8 for the two-section and single-section lasers, respectively, which indicate chirped pulses. AC traces corresponding to the shortest attainable pulsewidths in both the single- and two-section devices are shown in Fig. 7, obtained for driving currents of 200 mA and 100 mA (at a bias of 0.2 V) yielding ∼5.5 and ∼ 2.5 ps, respectively. For the optical spectrum, the general trend is an increase in the FWHM by decreasing the absorber bias down to an optimum value for a given driving current, as can be seen from Fig. 6(d) at $I =$ 180 mA. The spectral width also increases with drive current, as can be observed in Fig. 6(f) for a fixed absorber bias of −0.7 V. Fig. 6(f) also shows a similar trend for the single-section laser. We attribute this spectral enlargement for both the single- and two-section configurations to band-filling effects due to larger

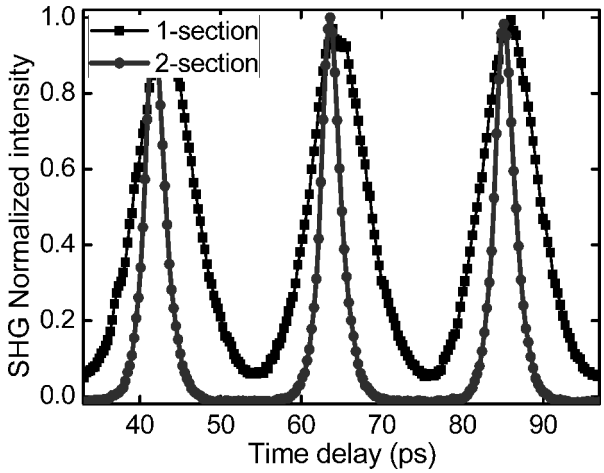

Fig. 7. AC traces for the single- and two-section devices when operating at 200 mA and [100 mA, 0.2 V], respectively.

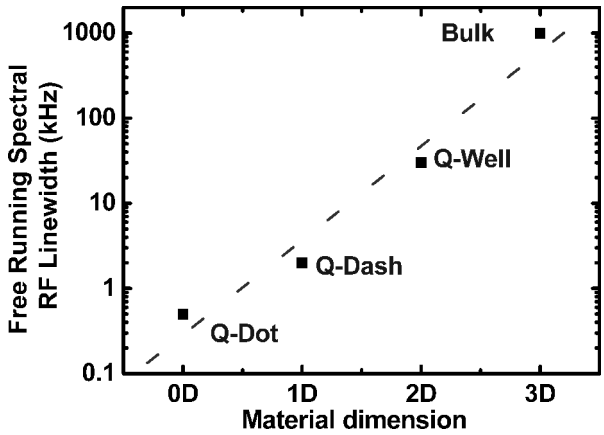

Fig. 8. RF linewidth dependence on material dimensionality. (Adapted from [7].)

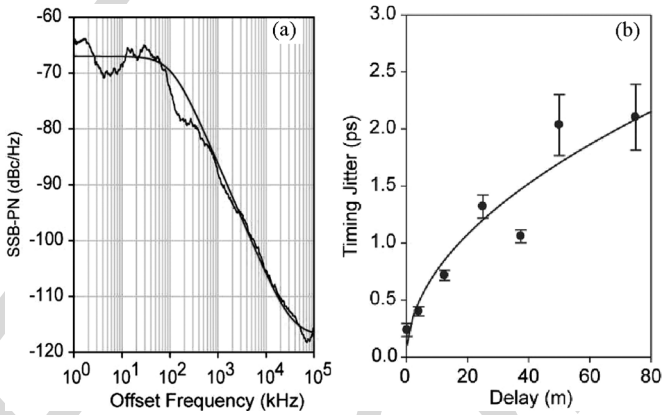

Fig. 9. (a) SSBPN spectral density around the first harmonic of the detected RF signal. (b) Evolution of the timing jitter with increasing delay in the cross-correlation measurement. Solid line: theoretical square-root fit. Reprinted with permission from [14].

carrier densities attainable in this nine-QDash layer active stack. Broad spectral features are desirable for applications such as coherent frequency comb generation for WDM transmission [18]. Both two-section and single-section devices when driven at high injection currents may hence be suitable for this kind of applications. Noise properties were assessed by measuring the RF linewidth of the first harmonic at 48 GHz. Both the single- and the two-section devices exhibited minimum RF linewidths of $\sim$100 kHz.

V. Noise in QDash Passive MLLs

A. Noise in Single-Section QDash Passive MLLs

MLLs are attractive candidates for the generation of stable and periodic pulse trains. They exhibit a potential for applications where small timing jitter is needed. For instance, optical sampling requires a timing jitter of less than 1 ps and even challenging values of 20 fs pulse-to-pulse for an 8-bit 40-Gb/s optical sampler [32]. MLLs characteristics are also potentially valuable in the realization of low-phase-noise oscillators at multigigahertz frequencies for applications in RoF systems [33]. For these purposes, low-dimension QD/Dash-based active materials exhibit unique properties compared to their QW-based counterparts. Indeed, the reduction of the material dimensionality, which implies a lower active volume, results in a lower optical confinement factor [3]; hence, the interaction of the optical guided mode with the ASE is reduced. Moreover, owing to the discrete nature of energy states, the energy diagram of a QD/Dash laser is equivalent to a three-level system [34], where the population inversion factor is close to one. These two properties are responsible for the improved timing jitter performance observed in QD/Dash MLLs. In passively MLLs, the frequency noise of the fundamental harmonic line, measured after photodetection, is mainly induced by spontaneous emission, which represents a source of frequency white noise or equivalently $1/f^2$ phase noise; therefore, the power spectral density of the photocurrent (RF spectrum) is given by a Lorentzian function, whose linewidth is found to be directly linked to the timing jitter [35]. It was shown that the value of the RF linewidth, and therefore, timing jitter, of an MLL is strongly affected by the material system and typically decreases by one order of magnitude when going from bulk to QW and from QW to QD/QDash active regions [7]. Typical values of the RF linewidth lie in the range of a few tens of kilohertz [13] down to a few hundreds of hertz [36], [37] for QD/QDash MLLs compared to several megahertz down to several hundreds of kilohertz for multi-QW MLLs (see Fig. 8), which indicate better timing jitter performance for the QD/Dash-based MLLs.

The timing jitter of passively MLLs is usually evaluated by integrating the single sideband phase noise (SSBPN) spectra in the RF domain. By using this technique, we have measured the timing jitter of single-section QDash MLLs with repetition frequencies of 40 and 10 GHz. The 40-GHz laser is based on a nine-layer InAs/InP DWELL structure. The SSBPN spectrum $L(f)$ measured by an electrical spectrum analyzer and its Lorentzian fit are represented in Fig. 9(a). Integration of the SSBPN was performed between 1 and 20 MHz. Below 1 MHz, the phase noise is affected by low-frequency drifts, and above 20 MHz, by the noise floor level of the ESA as described in [14].

The timing jitter amounts to 0.79 ps, obtained from the measured data, and 0.86 ps using a Lorentzian fit. Its RF linewidth was measured to be 240 kHz.

More recently, optimized active cores with a lower confinement factor have allowed a further reduction in the RF linewidth [37]. These active cores consist of a three-layer stack of InAs QDashes embedded in 40-nm-thick InGaAsP barriers. From this structure, a 10-GHz MLL was processed. A narrow RF linewidth of ∼850 Hz was obtained, leading to a timing jitter of 400 fs in the 150 kHz–50 MHz frequency range. The earlier measurement scheme presents a limitation in determining high-frequency jitter. The limitation arises from the noise floor of the electrical spectrum analyzer, which is reached at some point when increasing the offset frequency. Another limitation comes from the detector and the spectrum analyzer bandwidths, typically around 50 GHz, limiting the repetition frequency range of operation. These limitations are overcome by optical cross-correlation measurements, as described in [38]. This technique has been implemented for measuring the timing jitter in the previously described devices. The experimental setup is presented in [14]. The approach makes use of variable lengths of dispersion-shifted fiber and a controlled fine-delay stage with a 5-fs resolution. Fig. 9(b) shows the evolution of the integrated timing jitter τ_J with increasing delay in the cross-correlation measurement for the 40-GHz MLL. By fitting the data with a square-root function, the timing jitter is found to scale as $\tau_J = 0.201\ L^{1/2}$, with τ_J in units of picoseconds and L in units of meters. The length dependence of τ_J corresponds to the theoretical $1/f^2$ slope of the phase noise in passively MLLs. A timing jitter of 1.08 ps for the frequency interval [1 MHz, 20 MHz] has been evaluated, which is slightly larger than the value of 0.86 ps earlier found by integrating the first harmonic sideband. This technique was also applied to the optimized 10-GHz QDash MLL. A timing jitter of 500 fs in the 150 kHz–50 MHz range has been obtained, which is in good agreement with the value of 400 fs found after SSBPN integration [37].

In this section, we have demonstrated that InAs/InP QDash passive MLLs can exhibit narrow RF linewidths down to less than 1 kHz, implying subpicosend timing jitter values. These remarkable noise performances have been exploited for very high bit rate all-optical signal processing and can be used for low-noise millimeter-wave generation such as in RoF transmission systems (see Section VI).

B. Noise in Two-Section QDash Passive MLLs

First systematic investigations of two-section QDash passive MLLs emitting at 1.5 μm were presented in Section IV for an optimized DBAR structure. Noise trends as a function of driving conditions in these 48-GHz devices were assessed by RF linewidth measurements and compared to those of a one-section device from the same wafer and having same cavity length. Fig. 10(a) shows the dependence of the RF linewidth on the applied bias at currents of 120, 160, and 200 mA. A decrease in the RF linewidth with increasing reverse bias up to an optimum bias point is observed for a given drive current.

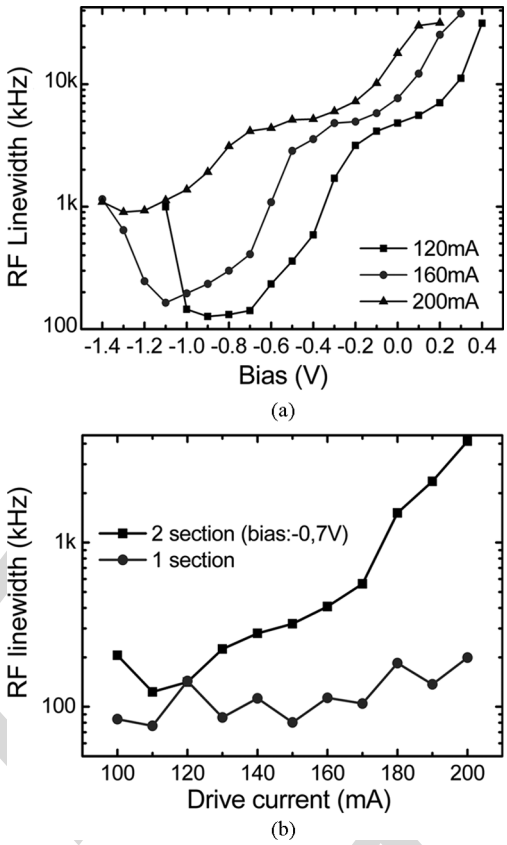

Fig. 10. RF linewidth as a function of (a) absorber bias and (b) driving current.

Fig. 10(b) shows the evolution of the RF linewidth as a function of driving current for both the single- and the two-section devices, the latter when biased at −0.7 V. We note an increase in the RF linewidth with current for the two-section device and a slight change for the one-section laser. These observations may be explained by recognizing that varying the gain section current or the absorber section bias outside their optimal range will alter the balance condition between the effects of gain saturation and saturable absorber that is required for mode locking in two-section devices; hence, a further increase or decrease in bias will result in unstable ML or CW regimes that can be evidenced by an increase in RF linewidth. The RF linewidth increase with current may be attributed to the optical spectrum broadening which results in a scale of ASE spectral bandwidth, and hence, ASE noise, thus increasing the timing phase noise. In general, the one-section device presents a reduced RF linewidth, which may be attributed to lower cavity losses, and hence, reduced phase noise from spontaneous emission. The generally larger RF linewidth observed in two-section devices can, however, be reduced by feedback-stabilization techniques without greatly affecting the pulse durations as described in the following section.

C. Noise Reduction in QDash Passive MLLs

The phase noise of QDash MLLs can be further reduced by means of stabilization techniques based on controlled feedback.

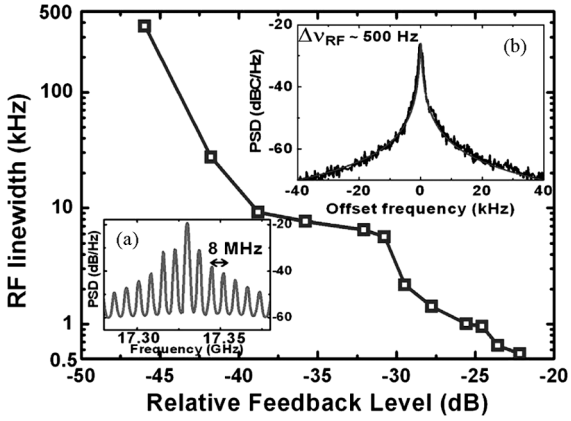

Fig. 11. RF linewidth as a function of the feedback level at a current of 110 mA and a voltage of –1.9 V. Inset (a) RF Spectrum showing harmonic modes separated by 8 MHz. Inset (b) RF spectrum with approximately −22 dB showing an RF linewidth of ∼500 Hz. Reprinted with permission from [40].

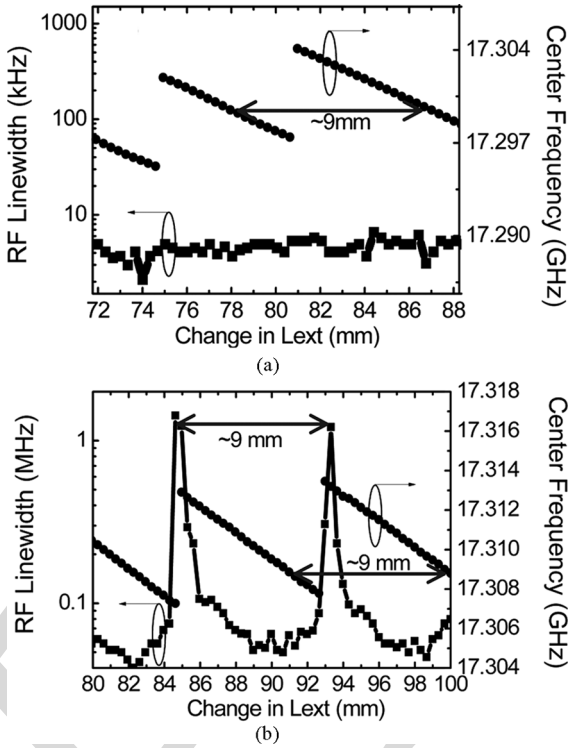

Fig. 12. RF linewidth and center frequency versus external cavity length change for (a) feedback level of approximately −22 dB and (b) feedback level of approximately −40 dB.

This approach has been applied to single-section devices using optoelectronic [19] and optical injection [39] schemes. It has also proven effective in reducing the RF linewidth in conventional two-section QDash MLLs [40] and more recently in InAs/GaAs QD MLLs [41] through optical feedback by using an external optical reflector. In particular, we have investigated the effect of external optical feedback on the pulse duration and RF linewidth of two-section passively MLLs at 17 GHz [40]. In this case, the active region consists of six layers of InAs QDashes. The absorber–gain length ratio of the laser is 4%. We measured the pulse duration and the RF linewidth as a function of gain current and reverse bias with no feedback and under variable feedback levels. Without feedback, pulse duration ranges from 3 to 14 ps, the shortest values being obtained for currents just above threshold. When the laser is subject to a maximum optical feedback of approximately –22 dB, stable mode locking is still observed, even though a reduction of 25% of the mode locking area is evidenced. Without optical feedback, the RF linewidth ranges from 250 kHz to 3.5 MHz. Under the effect of optical feedback, the RF linewidth decreases with feedback level. For instance, for a bias current of 110 mA and a reverse voltage of –1.9 V, the RF linewidth is reduced from 370 kHz (without feedback) down to a record value of 500 Hz with maximum feedback (see Fig. 11), implying a 27-timing jitter reduction [35]. This RF linewidth is comparable to that of high-performance InAs/GaAs QD MLLs [36].

We have also studied the effect of the external cavity length $L_{\rm ext}$ on the RF spectrum by using a delay stage in free space. At strong feedback levels greater than approximately −25 dB, the RF linewidth does not significantly change with $L_{\rm ext}$ [see Fig. 12(a)], whereas at lower feedback ratios [see Fig. 12 (b)], a ∼9-mm periodic dependence is observed. This length introduces a time delay of ∼60 ps in free space, which corresponds to the ML repetition frequency of 17 GHz. This periodicity may suggest an agreement with numerical simulations in [42] where the nonresonant case (i.e., when the ratio between $L_{\rm ext}$ and the laser cavity is irrational) would correspond to the regions of increased RF linewidth in Fig. 12(a). This case may also agree to the unstable dynamics observed by [43] in an InAs/GaAs QD MLL. Fig. 12 also shows the effect on the ML center frequency, showing a periodic dependence also reported in [43].

VI. Highlight of a Few Applications

Owing to their relatively low phase noise characteristics, one-section QDash MLLs have drawn a lot of interest for diverse applications, such as all-optical signal processing and low-noise optoelectronic oscillators (OEOs). Moreover, the wide optical spectrum features combined with the ML performance in these devices represent an advantage in the generation of optical frequency combs. This section reviews published literature related to some of these applications. It is to be noted that these are all single-section MLL-based applications, since high-performance mode locking in two-section devices at 1.5 μm have not been reported up to now.

A. High Bit Rate All-Optical Signal Processing.

All-optical clock recovery at 40 Gb/s has been recently achieved by using a single-section QDash MLL having a repetition frequency of 39.4 GHz [16]. High-frequency jitter suppression of a jittered signal is effectively achieved after injection into the QDash MLL owing to its inherently narrow free-running RF linewidth, which is measured to be 20 kHz when biased at 210 mA. The rms timing jitter of the input signal is reduced from 1.37 to 0.31 ps. The jitter filtering characteristics comply with the ITU-T recommendations. This result paves the way to all-optical clock recovery up to 160 Gb/s.

More recently, all-optical clock recovery performance have been measured at 40, 80, and 160 Gb/s through subharmonic locking mechanism in a 40-GHz one-section QDash FP laser exhibiting a narrow RF linewidth of 10 kHz [17]. Additionally, QDash passively MLLs have been used in wavelength preserving all-optical 3R regenerators at 40 Gb/s [44]. The 3R regenerator includes a single-section QDash MLL laser for low timing jitter clock recovery, which reduces the timing jitter of the input signal from 900 fs to an output timing jitter of less than 550 fs owing to the high-frequency noise-suppression characteristics of the QDash MLL. It is found that the timing jitter of the recovered clock does not change appreciably, as it remains constant at 350 fs for input timing jitters ranging from 400 to 900 fs.

B. Frequency Comb Generation

The inherently wide optical gain spectra related to the inhomogeneous broadening in QDash structures is an asset for frequency comb generation [45]. In addition, the perfect longitudinal mode spacing in QDash MLLs can offer the precise channel separation required in WDM systems, which is otherwise difficult to accomplish. Moreover, due to the ML process, the WDM channels will be coherent, leading to a reduced crosstalk and to an optimal spectral efficiency [46]**.** Error-free transmission of eight separate channels has recently been achieved at 10 Gb/s for a 50-km SMF span, using a 100-GHz QDash-based MLL [18] having a flat optical spectrum of $\sim$10 nm width. The 100-GHz spaced channels are filtered out and launched separately into the fiber. A small measured penalty of $\sim$1.5 dB by using this transmission scheme is shown to arise from the higher relative intensity noise of single longitudinal modes. Bandgap engineering of QDash structures to further widen the optical spectrum remains a key strategy to continue increasing the capacity of WDM systems.

C. Radio Over Fiber

QDash-based MLLs present interesting properties and potential for 60-GHz RoF systems for broadband wireless services. The increase in the demand of bandwidth-hungry multiple services (e.g., multimedia applications such as high-definition TV (HDTV) at bit rates from 1 Gb/s up to 10 Gb/s per user requires the use of transmission techniques of millimeter-wave signals over optical fibers [33], [47].

To ascertain the validity of QDash MLLs for wireless networks, experiments of both frequency up-conversion and distribution, and frequency down-conversion and distribution were carried out over several tens of meters. The radio signal is taken from the IEEE 802 standard [47] with a data rate of 3 Gb/s. The mean error vector magnitude (EVM) was measured to be 10.5% and 15.2% for the up- and down-conversion processes, respectively. The criterion for successful detection being an EVM less than 23%, these experiments validate the ability of the use of single-section QDash lasers for radio-signal transport.

The advantages of 60-GHz QDash MLLs were further assessed in transmission experiments of uncompressed HDTV at a maximum data rate of 3 Gb/s, another major application of broadband RoF technology. It is worth noting that the generation unit consists of a single 60-GHz MLL that can be directly modulated to encode the data onto the signal.

Further improvement of the performances includes the optimization of the direct modulation bandwidth. This implies a simultaneous optimization of the active region for both enhanced mode-locking efficiency and increased direct modulation bandwidth. Such devices are expected to offer a very competitive approach for compact, reduced complexity and cost-effective systems for millimeter-wave generation at the central station for bit rates beyond 10 Gb/s compared to systems using a Mach–Zehnder modulator.

D. Low-Phase-Noise-Coupled Optoelectronic Oscillator

QDash passively MLLs have also been used for the realization of low noise OEOs for millimeter-wave generation [19], [39]. A first demonstration based on a coupled OEO used a 39.9-GHz single-section MLL inserted into two fiber loops. The optical signal is detected by a high-speed photodiode and the resulting electrical signal is fed back into the laser through a bias tee [19]. When the loop is closed, the phase noise is efficiently reduced from –55 dB·c/Hz to –75dB·c/Hz at an offset of 10 kHz and from –75 kHz to –94 dB–c/Hz at an offset of 100 kHz. As the –3-dB modulation bandwidth of the laser was less than 3 GHz, further improvement of the phase noise to comply with system requirements implies reducing the losses of the loops by increasing the modulation efficiency of the QDash laser. As mentioned in part C, practical applications force to perform specific growth optimization both for improved nonlinear effects (i.e., enhanced FWM efficiency) and increased differential gain.

More recently, low phase noise OEO was implemented by means of a 10-GHz QD MLL (RF linewidth $<$ 30 kHz) integrated into a self-injection loop [39]. This makes the whole system simpler and potentially more compact compared to the optoelectronic oscillator that makes use of optoelectronic conversion. When the loop is open, the phase noise exhibits a typical value of –75 dB·c/Hz at an offset of 100 kHz and when the loop is closed its value is reduced to –105 dB·c/Hz, a $\sim$30-dB phase noise reduction. This demonstrates the potential of QDash MLLs inserted into a controlled feedback loop to achieve low-noise oscillators without optoelectronic conversion.

VII. Conclusion

Progress in the growth of self-assembled QDs and QDashes on InP semiconductor substrates has allowed the achievement of high-performance long-wavelength monolithic MLLs. Specific QDash properties, such as inhomogeneous broadening, fast carrier dynamics, and low optical confinement factors have proved valuable assets for ultrashort pulse generation with extremely low noise. Single-section QDash-based FP devices in particular have demonstrated subpicosecond pulsewidths at ultrahigh repetition rates up to 346 GHz. RF linewidths down to a few kilohertz have been reported. Subpicosecond timing jitter in 10- and 40-GHz single-section MLLs was obtained. Controlled optical feedback has allowed to further decrease the RF linewidth to the sub-kHz range in the more standard two-section MLL configuration. There is still room for performance

improvement by fully exploiting the broad optical spectrum. The influence of the type of active region (e.g., DWELL or DBAR) on mode-locking performance will be further investigated. Future developments should also include output power optimization in specific (flared) guided wave configurations.

This should pave the way to a number of applications in the field of not only optical telecommunications but also optical interconnects or microwave photonics. First reported demonstrations based on one-section devices include all-optical clock recovery at up to 160 Gb/s, generation of coherent frequency combs for high bit rate WDM transmission, RoF at 60 GHz for broadband wireless services and extremely low phase noise in all-optical oscillators.

REFERENCES

[1] E. Avrutin, J. Marsh, and E. Portnoi, "Monolithic and multi-GigaHertz mode-locked semiconductor lasers: Constructions, experiments, models and applications," in *Proc. Inst. Elect. Eng., Optoelectron.*, 2000, vol. 147, pp. 251–278.

[2] K. A. Williams, M. G. Thompson, and I. H. White, "Long-wavelength monolithic mode-locked diode lasers," *New J. Phys.*, vol. 6, p. 179, 2004.

[3] D. Bimberg, N. Kirstaedter, N. N. Ledentsov, Z. I. Alferov, P. Kop'ev, and V. M. Ustinov, "InGaAs-GaAs quantum-dot lasers," *IEEE J. Sel. Topics Quantum Electron.*, vol. 3, no. 2, pp. 196–205, Apr. 1997.

[4] X. Huang, A. Stintz, H. Li, L. F. Lester, J. Cheng, and K. J. Malloy, "Passive mode-locking in 1.3 μm two-section InAs quantum dot lasers," *Appl. Phys. Lett.*, vol. 78, pp. 2825–2827, May 2001.

[5] E. U. Rafailov, M. A. Cataluna, and W. Sibbett, "Mode-locked quantum-dot lasers," *Nat. Photon.*, vol. 1, pp. 395–401, Jul. 2007.

[6] M. G. Thompson, A. Rae, X. Mo, R. V. Penty, and I. H. White, "InGaAs quantum-dot mode-locked laser diodes," *IEEE J. Sel. Topics Quantum Electron.*, vol. 15, no. 3, pp. 661–672, Jun. 2009.

[7] F. Lelarge, B. Dagens, J. Renaudier, R. Brenot, A. Accard, F. van Dijk, D. Make, O. Le Gouezigou, J. Provost, F. Poingt, J. Landreau, O. Drisse, E. Derouin, B. Rousseau, F. Pommereau, and G. Duan, "Recent advances on InAs/InP quantum dash based semiconductor lasers and optical amplifiers operating at 1.55 μm," *IEEE J. Sel. Topics Quantum Electron.*, vol. 13, no. 1, pp. 111–124, Jan./Feb. 2007.

[8] R. H. Wang, A. Stintz, P. M. Varangis, T. C. Newell, H. Li, K. J. Malloy, and L. F. Lester, "Room-temperature operation of InAs quantum-dash lasers on InP [001]," *IEEE Photon. Technol. Lett.*, vol. 13, no. 8, pp. 767–769, Aug. 2001.

[9] R. Schwertberger, D. Gold, J. P. Reithmaier, and A. Forchel, "Long-wavelength InP-based quantum-dash lasers," *IEEE Photon. Technol. Lett.*, vol. 14, no. 6, pp. 735–737, Jun. 2002.

[10] Z. G. Lu, J. R. Liu, S. Raymond, P. J. Poole, P. J. Barrios, and D. Poitras, "312-fs pulse generation from a passive C-band InAs/InP quantum dot mode-locked laser," *Opt. Exp.*, vol. 16, pp. 10835–10840, Jul. 2008.

[11] M. J. R. Heck, E. A. J. M. Bente, B. Smalbrugge, Y. Oei, M. K. Smit, S. Anantathanasarn, and R. Notzel, "Observation of Q-switching and mode-locking in two-section InAs/InP (100) quantum dot lasers around 1.55 μm," *Opt. Exp.*, vol. 15, pp. 16292–16301, Dec. 2007.

[12] J. Renaudier, R. Brenot, B. Dagens, F. Lelarge, B. Rousseau, F. Poingt, O. Legouezigou, F. Pommereau, A. Accard, P. Gallion, and G. Duan, "45 GHz self-pulsation with narrow linewidth in quantum dot Fabry-Perot semiconductor lasers at 1.5 μm," *Electron. Lett.*, vol. 41, pp. 1007–1008, 2005.

[13] C. Gosset, K. Merghem, A. Martinez, G. Moreau, G. Patriarche, G. Aubin, A. Ramdane, J. Landreau, and F. Lelarge, "Subpicosecond pulse generation at 134 GHz using a quantum-dash-based Fabry-Perot laser emitting at 1.56 μm," *Appl. Phys. Lett.*, vol. 88, pp. 241105–241113, Jun. 2006.

[14] J. P. Tourrenc, A. Akrout, K. Merghem, A. Martinez, F. Lelarge, A. Shen, G. H. Duan, and A. Ramdane, "Experimental investigation of the timing jitter in self-pulsating quantum-dash lasers operating at 1.55 μm," *Opt. Exp.*, vol. 16, pp. 17706–17713, Oct. 2008.

[15] C. Gosset, K. Merghem, G. Moreau, A. Martinez, G. Aubin, J. Oudar, A. Ramdane, and F. Lelarge, "Phase-amplitude characterization of a high-repetition-rate quantum dash passively mode-locked laser," *Opt. Lett.*, vol. 31, pp. 1848–1850, Jun. 2006.

[16] J. Renaudier, B. Lavigne, F. Lelarge, M. Jourdran, B. Dagens, O. Legouezigou, P. Gallion, and G. Duan, "Standard-compliant jitter transfer function of all-optical clock recovery at 40 GHz based on a quantum-dot self-pulsating semiconductor laser," *IEEE Photon. Technol. Lett.*, vol. 18, no. 11, pp. 1249–1251, Jun. 2006.

[17] V. Roncin, A. O'Hare, S. Lobo, E. Jacquette, L. Bramerie, P. Rochard, Q. Le, M. Gay, J. Simon, A. Shen, J. Renaudier, F. Lelarge, and G. Duan, "Multi-data-rate system performance of a 40-GHz all-optical clock recovery based on a quantum-dot fabry-PÉrot laser," *IEEE Photon. Technol. Lett.*, vol. 19, no. 19, pp. 1409–1411, Oct. 2007.

[18] A. Akrout, A. Shen, R. Brenot, F. Van Dijk, O. Legouezigou, F. Pommereau, F. Lelarge, A. Ramdane, and G. Duan, "Separate error-free transmission of eight channels at 10 Gb/s using comb generation in a quantum-dash-based mode-locked laser," *IEEE Photon. Technol. Lett.*, vol. 21, pp. 1746–1748, 2009.

[19] F. van Dijk, A. Enard, X. Buet, F. Lelarge, and G. Duan, "Phase noise reduction of a quantum dash mode-locked laser in a millimeter-wave coupled opto-electronic oscillator," *J. Lightw. Technol.*, vol. 26, no. 15, pp. 2789–2794, Aug. 2008.

[20] G. Moreau, S. Azouigui, D. Cong, K. Merghem, A. Martinez, G. Patriarche, A. Ramdane, F. Lelarge, B. Rousseau, B. Dagens, F. Poingt, A. Accard, and F. Pommereau, "Effect of layer stacking and p-type doping on the performance of InAs/InP quantum-dash-in-a-well lasers emitting at 1.55 μm," *Appl. Phys. Lett.*, vol. 89, pp. 241123–241125, Dec. 2006.

[21] A. Martinez, G. Aubin, F. Lelarge, R. Brenot, J. Landreau, and A. Ramdane, "Variable optical delays at 1.55 mu m using fast light in an InAs/InP quantum dash based semiconductor optical amplifier," *Appl. Phys. Lett.*, vol. 93, pp. 091116–091118, 2008.

[22] A. Capua, S. O'Duill, V. Mikhelashvili, G. Eisenstein, J. P. Reithmaier, A. Somers, and A. Forchel, "Cross talk free multi channel processing of 10 Gbit/s data via four wave mixing in a 1550 nm InAs/InP quantum dash amplifier," *Opt. Exp.*, vol. 16, pp. 19072–19077, Nov. 2008.

[23] K. Sato, "Optical pulse generation using fabry-Perot lasers under continuous-wave operation," *IEEE J. Sel. Topics Quantum Electron.*, vol. 9, no. 5, pp. 1288–1293, Sep./Oct. 2003.

[24] Y. Nomura, S. Ochi, N. Tomita, K. Akiyama, T. Isu, T. Takiguchi, and H. Higuchi, "Mode locking in Fabry-Perot semiconductor lasers," in *Phys. Rev. A*, Mar. 2002, vol. 65, pp. 043807–043817.

[25] K. Merghem, A. Akrout, A. Martinez, G. Aubin, A. Ramdane, F. Lelarge, and G. Duan, "Pulse generation at 346 GHz using a passively mode locked quantum-dash-based laser at 1.55μm," *Appl. Phys. Lett.*, vol. 94, p. 021107, 2009.

[26] Y. C. Xin, Y. Li, V. Kovanis, A. L. Gray, L. Zhang, and L. F. Lester, "Reconfigurable quantum dot monolithic multisection passive mode-locked lasers," *Opt. Exp.*, vol. 15, pp. 7623–7633, Jun. 2007.

[27] H. Schmeckebier, G. Fiol, C. Meuer, D. Arsenijevi, and D. Bimberg, "Complete pulse characterization of quantum dot mode-locked lasers suitable for optical communication up to 160 Gbit/s," *Opt. Exp.*, vol. 18, pp. 3415–3425, Feb. 2010.

[28] M. J. Heck, E. J. Salumbides, A. Renault, E. A. Bente, Y. Oei, M. K. Smit, R. van Veldhoven, R. Notzel, K. S. Eikema, and W. Ubachs, "Analysis of hybrid mode-locking of two-section quantum dot lasers operating at 1.5 μm," *Opt. Exp.*, vol. 17, pp. 18063–18075, 2009.

[29] C. Lin, Y. Xin, Y. Li, F. L. Chiragh, and L. F. Lester, "Cavity design and characteristics of monolithic long-wavelength InAs/InP quantum dash passively mode-locked lasers," *Opt. Exp.*, vol. 17, pp. 19739–19748, Oct. 2009.

[30] D. B. Malins, A. Gomez-Iglesias, S. J. White, W. Sibbett, A. Miller, and E. U. Rafailov, "Ultrafast electroabsorption dynamics in an InAs quantum dot saturable absorber at 1.3 μm," *Appl. Phys. Lett.*, vol. 89, pp. 171111–171113, 2006.

[31] G. Fiol, C. Meuer, H. Schmeckebier, D. Arsenijevic, S. Liebich, M. Laemmlin, M. Kuntz, and D. Bimberg, "Quantum-Dot semiconductor mode-locked lasers and amplifiers at 40 GHz," *Quantum Electron., IEEE J.*, vol. 45, no. 11, pp. 1429–1435, Nov. 2009.

[32] P. Juodawlkis, J. Twichell, G. Betts, J. Hargreaves, R. Younger, J. Wasserman, F. O'Donnell, K. Ray, and R. Williamson, "Optically sampled analog-to-digital converters," *IEEE Trans. Microw. Theor. Tech.*, vol. 49, no. 10, pp. 1840–1853, Oct. 2001.

[33] A. Vieira, P. Herczfeld, A. Rosen, M. Ermold, E. Funk, W. Jemison, and K. Williams, "A mode-locked microchip laser optical transmitter for fiber radio," *IEEE Trans. Microw. Theor. Tech.*, vol. 49, no. 10, pp. 1882–1887, Oct. 2001.

[34] T. W. Berg and J. Mørk, "Quantum dot amplifiers with high output power and low noise," *Appl. Phys. Lett.*, vol. 82, pp. 3083–3085, 2003.

[35] F. Kefelian, S. O'Donoghue, M. T. Todaro, J. G. McInerney, and G. Huyet, "RF linewidth in monolithic passively mode-locked semiconductor laser," *IEEE Photon. Technol. Lett.*, vol. 20, no. 16, pp. 1405–1407, Aug. 2008.
[36] G. Carpintero, M. G. Thompson, R. V. Penty, and I. H. White, "Low noise performance of passively mode-locked 10-GHz quantum-dot laser diode," *IEEE Photon. Technol. Lett.*, vol. 21, no. 6, pp. 389–391, Mar. 2009.
[37] A. Akrout, K. Merghem, J. P. Tourrenc, A. Martinez, A. Shen, F. Lelarge, G. H. Duan, and A. Ramdane, "Generation of 10 GHz optical pulses with very low timing jitter using one section passively mode locked quantum dash based lasers operating at 1.55 μm," presented at the Opt. Fiber Commun. Conf./Nat. Fiber Opt. Eng. Conf., San Diego, CA, 2009.
[38] L. Jiang, M. Grein, H. Haus, and E. Ippen, "Noise of mode-locked semiconductor lasers," *IEEE J. Sel. Topics Quantum Electron.*, vol. 7, no. 2, pp. 159–167, Apr. 2001.
[39] A. Akrout, A. Shen, A. Enard, G. Duan, F. Lelarge, and A. Ramdane, "Low phase noise all-optical oscillator using quantum dash modelocked laser," *Electron. Lett.*, vol. 46, pp. 73–74, Jan. 2010.
[40] K. Merghem, R. Rosales, S. Azouigui, A. Akrout, A. Martinez, F. Lelarge, G. Duan, G. Aubin, and A. Ramdane, "Low noise performance of passively mode locked quantum-dash-based lasers under external optical feedback," *Appl. Phys. Lett.*, vol. 95, pp. 131111–131113, 2009.
[41] C. Y. Lin, F. Grillot, N. A. Naderi, Y. Li, and L. F. Lester, "Rf linewidth reduction in a quantum dot passively mode-locked laser subject to external optical feedback," *Appl. Phys. Lett.*, vol. 96, pp. 051118–051120, Feb. 2010.
[42] E. A. Avrutin and B. M. Russell, "Dynamics and spectra of monolithic mode-locked laser diodes under external optical feedback," *IEEE J. Quantum Electron.*, vol. 45, no. 11, pp. 1456–1464, Nov. 2009.
[43] F. Grillot, C.-Y. Lin, N. A. Naderi, M. Pochet, and L. F. Lester, "Optical feedback instabilities in a monolithic InAs/GaAs quantum dot passively mode-locked laser," *Appl. Phys. Lett.*, vol. 94, pp. 153503–153505, 2009.
[44] X. Tang, S. H. Chung, J. C. Cartledge, A. Shen, A. Akrout, and G. Duan, "Application of a passively mode-locked quantum-dot Fabry-Perot laser in 40 Gb/s all-optical 3R regeneration," *Opt. Exp.*, vol. 18, pp. 9378–9383, Apr. 2010.
[45] A. Gubenko, I. Krestnikov, D. Livshtis, S. Mikhrin, A. Kovsh, L. West, C. Bornholdt, N. Grote, and A. Zhukov, "Error-free 10 Gbit/s transmission using individual Fabry-Perot modes of low-noise quantum-dot laser," *Electron. Lett.*, vol. 43, pp. 1430–1431, 2007.
[46] T. Healy, F. C. Garcia Gunning, A. D. Ellis, and J. D. Bull, "Multi-wavelength source using low drive-voltage amplitude modulators for optical communications," *Opt. Exp.*, vol. 15, pp. 2981–2986, Mar. 2007.
[47] A. Stöhr, A. Akrout, R. Bub, B. Charbonnier, F. van Dijk, A. Enard, S. Fedderwitz, D. Jäger, M. Huchard, F. Lecoche, J. Marti, R. Sambaraju, A. Steffan, A. Umbach, and M. Weib, "60 GHz radio-over-fiber technologies for broadband wireless services [Invited]," *J. Opt. Netw.*, vol. 8, pp. 471–487, May. 2009.

Ricardo Rosales received the M.Sc. degree in electrical and optical engineering from Telecom SudParis, Evry, France, in 2009. He is currently working toward the Ph.D. degree at the Centre National de la Recherche Scientifique–Laboratory for Photonics and Nanostructures, Marcoussis, France.

His current research interests include semiconductor mode-locked lasers and quantum-dot laser diodes.

Kamel Merghem received the Master's degree in lasers and applications from Université des Sciences et Technologies, Lille, France, in 2000.

He is currently a Research Engineer at the Centre National de la Recherche Scientifique–Laboratory for Photonics and Nanostructures, Marcoussis, France, where he is involved in the research on the fabrication and characterization of semiconductor lasers for telecom applications. His research interests include mode-locked lasers and quantum-dot lasers.

Anthony Martinez was born in 1975. He received the Ph.D. degree in optoelectronics in 2002.

From 2003 to 2005, he was a Postdoctoral Fellow at the Laboratory for Photonics and Nanostructures, where he was the in charge of the design, fabrication and characterizations of high speed lasers based on novel material systems: GaInNAs/GaAs quantum wells and InAs/GaAs quantum dot material for emission at 1.3 μm, and InAs/InP quantum dots/dash operating at 1.55 μm. During 2005, he was a Postdoctoral Fellow at the Center For High Technology Materials (NM), where he was involved in the research on microwave frequency properties of quantum-dot-based lasers. Since 2006, he has been a Permanent Researcher at the Centre National de la Recherche Scientifique–Laboratory for Photonics and Nanostructures, Marcoussis, France. His research interests include photonics components, i.e., semiconductor-based lasers and amplifiers, for telecommunication and defense applications. He has published more than 35 papers in peer-reviewed journals.

A. Akrout, Photograph and biography not available at the time of publication.

J.-P. Tourrenc, Photograph and biography not available at the time of publication.

Alain Accard was born in France, in 1950. He received the M.S. engineer degree in physics from the Institut National des Sciences Appliquees, Lyon, France, in 1975.

He is currently engaged at Alcatel Thales III–V Laboratory, Marcoussis, France. His research interests include Bragg grating design and fabrication of Fabry–Perot and distributed feedback lasers.

Francois Lelarge was born in France, in 1966. He received the Diploma degree in material science and the Ph.D. degree from the University of Pierre et Marie Curie, Paris, France, in 1993 and 1996, respectively.

From 1993 to 1996, he was with the Laboratory of Microstructures and Microelectronic, Centre National de la Recherche Scientifique Bagneux, France. His thesis focused on the fabrication and the optical characterization of GaAs/AlAs lateral supperlattice grown on vicinal surfaces by molecular beam epitaxy. From 1997 to 2000, he was a Postdoctoral Researcher at the Institute of Micro and Optoelectronics, Lausanne, Switzerland, where he was involved in the research on InGaAs/GaAs quantum wires fabrication by metal–organic chemical vapor deposition regrowth on patterned substrates. Currently, he is at Alcatel Thales III–V Laboratory, Marcoussis, France, where he is involved in the research on InGaAsP/InP gas source MBE growth for optoelectronic devices, in particular, on quantum-dots-based lasers and amplifiers.

Abderrahim Ramdane received the Ph.D. degree in semiconductor physics from the University of Nottingham, Nottingham, U.K. in 1981.

He was a Postdoctoral Research Fellow at University of Nottingham for two years, where he was involved in the research on deep levels in III–V compounds. In 1983, he joined the Solar Material Laboratory in Algiers as the Head, where he was involved in the research on single crystal and amorphous silicon solar cells. In 1990, he joined FRANCE TELECOM/Centre National d'Etudes des Télécommunications (CNET Bagneux) as the In Charge of the " Photonic Integrated Circuits on InP" activity. Since 1999, he has been the Director of Research at Centre National de la Recherche Scientifique–Laboratory for Photonics and Nanostructures, Marcoussis, France, where he is engaged in the research on nanostructured optical devices. He has authored or coauthored more than 200 publications in peer reviewed journals and international conferences, and holds five patents in the field of optoelectronic devices.